Published in final edited form as:
Free Radic Biol Med. 2009 June 15; 46(12): 1614–1625. doi:10.1016/j.freeradbiomed.2009.03.016.

Distinct Nrf1/2-independent mechanisms mediate As3+-induced glutamate-cysteine ligase subunit gene expression in murine hepatocytes

James A. Thompson[1,7], **Collin C. White**[2], **David P. Cox**[2], **Jefferson Y. Chan**[3], **Terrance J. Kavanagh**[2], **Nelson Fausto**[1], and **Christopher C. Franklin**[4,5,6]

[1] Department of Pathology, University of Washington, Seattle, WA 98195

[2] Department of Environmental and Occupational Health Sciences, University of Washington, Seattle, WA 98195

[3] Department of Pathology and Laboratory Medicine, University of California-Irvine, Irvine, CA 92697

[4] Department of Pharmaceutical Sciences, School of Pharmacy, University of Colorado Denver, Aurora, CO 80045

[5] University of Colorado Cancer Center, University of Colorado Denver, Aurora, CO 80045

Abstract

Trivalent arsenite (As3+) is a known human carcinogen that is also capable of inducing apoptotic cell death. Increased production of reactive oxygen species is thought to contribute to both the carcinogenic and cytotoxic effects of As3+. Glutathione (GSH) constitutes a vital cellular defense mechanism against oxidative stress. The rate-limiting enzyme in GSH biosynthesis is glutamate-cysteine ligase (GCL), a heterodimeric holoenzyme composed of a catalytic (GCLC) and a modifier (GCLM) subunit. In this study, we demonstrate that As3+ coordinately upregulates *Gclc* and *Gclm* mRNA levels in a murine hepatocyte cell line resulting in increased GCL subunit protein expression, holoenzyme formation and activity. As3+ increased the rate of transcription of both the *Gclm* and *Gclc* genes and induced the post-transcriptional stabilization of *Gclm* mRNA. The antioxidant N-acetylcysteine abolished As3+-induced *Gclc* expression and attenuated induction of *Gclm*. As3+ induction of *Gclc* and *Gclm* was also differentially regulated by the MAPK signaling pathways and occurred independent of the Nrf1/2 transcription factors. These findings demonstrate that distinct transcriptional and post-transcriptional mechanisms mediate the coordinate induction of the *Gclc* and *Gclm* subunits of GCL in response to As3+ and highlight the potential importance of the GSH antioxidant defense system in regulating As3+-induced responses in hepatocytes.

Keywords

arsenite; arsenic; glutamate cysteine ligase; GCL; GCLC; GCLM; glutathione; GSH; hepatocyte; Nrf2; gene transcription

6To whom correspondence should be addressed: University of Colorado Denver, Department of Pharmaceutical Sciences, School of Pharmacy, C238-P15, Research-2, 12700 E. 19th Avenue, Room 3009, Aurora, CO 80045, phone: 303-724-6124, FAX: 303-724-7266, e-mail: christopher.franklin@ucdenver.edu.
[7]Current address: Midwestern University, Arizona College of Osteopathic Medicine, Glendale, AZ 85308

INTRODUCTION

Inorganic arsenic, as trivalent arsenite (As3+) or pentavalent arsenate (As5+), is a known human carcinogen associated with the development of cancers of the skin, bladder, lung, and kidney [1]. Chronic arsenic exposure is also associated with numerous liver pathologies, including hepatocellular carcinoma (HCC), liver angiosarcoma, hepatomegaly, fibrosis, and cirrhosis [2,3]. As3+ exhibits clear dose-dependent effects, with low levels promoting cell proliferation and transformation and higher concentrations inducing apoptosis [4]. In this regard, chronic exposure to sub-toxic doses of As3+ induces malignant transformation in multiple *in vitro* cell models, including rat liver epithelial cells [5], human bladder urothelial cells [6], human prostate cells [7], human keratinocytes [8,9], and mouse epidermal cells [10]. In contrast, acute exposure to high concentrations of As3+ induces apoptotic cell death, which provides the molecular basis for the therapeutic use of arsenic trioxide (ATO) in the treatment of acute promyelocytic leukemia [11]. While the molecular mechanisms mediating As3+-induced transformation and apoptosis have not been fully elucidated, increased production of reactive oxygen species (ROS) and aberrant gene expression have been implicated in both responses [11–13]. Interestingly, As3+-induced transformation *in vitro* is associated with the development of cellular resistance to acute As3+ toxicity [8,14–19], which is usually accompanied by an up-regulation of the glutathione (GSH) antioxidant defense system [8,15,19,20]. GSH plays an important role in arsenic detoxication and intracellular GSH levels can dictate cellular sensitivity to As3+-induced apoptosis [21]. Cells deficient in GSH biosynthesis or depleted of cellular GSH levels exhibit dramatically increased sensitivity to As3+-induced apoptosis [11,22,23], while enhanced cellular GSH levels promote resistance to As3+-induced apoptosis [11,21]. Both acute and chronic As3+ exposure up-regulate various antioxidant enzymes that likely serve a cytoprotective adaptive mechanism against As3+-induced oxidative stress, including enzymes of the GSH antioxidant defense system.

Mammalian cells possess a number of antioxidant defense mechanisms to counteract the deleterious effects of oxidative stress associated with exposure to environmental toxicants. GSH is the most abundant non-protein thiol in the cell and plays an important role in cellular defense against oxidative stress. The antioxidant and cytoprotective functions of GSH are derivative of its ability to directly react with reactive electrophiles, act as a cofactor in the reduction of both hydrogen peroxide (H_2O_2) and lipid peroxides mediated by glutathione peroxidases (GPx), and conjugation reactions mediated by glutathione S-transferases (GST) [24,25]. Non-enzymatic and GPx-mediated reduction reactions lead to the oxidation of GSH and formation of glutathione disulfide (GSSG), which is readily reduced by glutathione reductase (GR) to regenerate GSH [24]. In contrast, GST-mediated conjugation reactions usually result in a net loss of GSH due to multidrug resistance-associated protein (MRP)- and/or organic anion transporting polypeptide (OATP)-mediated export of the GSH-conjugate from the cell [26]. Failure to adequately replenish these depleted cellular GSH stores quickly compromises cellular redox homeostasis and cell viability. Most cells do not import significant quantities of GSH, highlighting the importance of *de novo* GSH biosynthesis in maintaining intracellular GSH levels during periods of GSH deficiency.

GSH is synthesized by two sequential ATP-dependent reactions catalyzed by glutamate cysteine ligase (GCL) and glutathione synthetase [24]. GCL is the first and rate-limiting step in GSH biosynthesis [24]. GCL is a heterodimeric holoenzyme consisting of a catalytic subunit (GCLC, 73 kDa), which contributes all the enzymatic activity and contains all the substrate binding sites of GCL, and a modifier subunit (GCLM, 31 kDa), which modulates GCLC activity and affinity for substrates and inhibitors [24,27]. GCLM increases the Vmax and Kcat of GCLC, lowers the Km for glutamate and ATP and increases the Ki for GSH feedback regulation of GCLC [24,27]. Thus, while GCLM does not retain any catalytic activity, GCL

holoenzyme formation is essential for optimal GCLC enzymatic activity under physiological concentrations of glutamate and GSH.

GSH biosynthesis can be rapidly regulated by increased expression of the GCL subunits via transcriptional, post-transcriptional, and/or translational control mechanisms or post-translational modification of pre-existing GCL protein [27,28]. Both GCL subunits are highly inducible and the relative levels of the GCL subunits are a major determinant of cellular GCL activity and GSH biosynthetic capacity [28]. In addition to inducing glutathione reductase and glutathione S-transferase expression and activity, acute exposure to subtoxic concentrations of As3+ induces *Gclc* gene expression and enhances GCL enzymatic activity in human keratinocytes and rat lung epithelial cells [29–31]. However, the molecular mechanisms mediating these responses are not known and it is not clear whether As3+ coordinately induces *Gclm* expression. Analysis of the *Gclc* and *Gclm* promoters reveal the presence of multiple regulatory elements that have been implicated in their inducible expression, including consensus AP-1, AP-2, ARE, SP1, and NF-κB response elements [28,32,33]. Nrf1, Nrf2 and p45-NFE2 are members of the Cap-n-collar bZIP transcription factor family that play an important role in the expression of phase II detoxication and antioxidative enzymes [34]. Nrf1 and Nrf2 are ubiquitously expressed, while p45-NFE2 expression is restricted to hematopoietic cells [34]. Nrf1 and Nrf2 are central mediators in the constitutive and inducible expression of the *Gcl* subunits in response to oxidative stress through activation of antioxidant response elements (ARE) [35,36]. Additional transcription factors have also been implicated in mediating the inducible expression of *Gclc* and *Gclm*, including members of the Jun, Fos, ATF-2, MTF-1 and CREB family of proteins [32]. Importantly, As3+ activates Nrf1/2 as well as the MAPK pathways that activate these transcription factors and regulate *Gclc* and *Gclm* gene expression [9,30,37–41].

In this study, we examined the molecular mechanisms and signal transduction pathways regulating As3+-induced GCL subunit expression in the TAMH murine hepatocyte cell line. While As3+ coordinately induced *Gclc* and *Gclm* gene expression, distinct transcriptional and post-transcriptional regulatory mechanisms mediated these responses. Surprisingly, while Nrf1 and Nrf2 are known to regulate both constitutive and inducible *Gclc* and *Gclm* expression, neither was required for As3+-induced *Gclc* or *Gclm* expression. Rather, our studies indicate that the p38 MAPK and ERK pathway play a prominent role in mediating As3+-induced *Gcl* subunit gene expression. These transcriptional events are also functionally relevant as As3+ increased GCLC and GCLM protein expression and GCL enzymatic activity. In aggregate, these studies identify many of the transcriptional and post-transcriptional mechanisms and signal transduction pathways that regulate As3+-induced *Gcl* subunit gene expression, GCL activity and GSH biosynthetic capacity in murine hepatocytes.

MATERIALS AND METHODS

Reagents

$NaAsO_2$, Na_2HAsO_4, N-acetylcysteine (NAC), cycloheximide (CHX), buthionine sulfoximine (BSO), and *tert*-butylhydroquinone (tBHQ) were purchased from Sigma Chemical Co. (St. Louis, MO). Actinomycin D (ActD) was purchased from Calbiochem (La Jolla, CA). SB202190, SP600125, PD98059, and the JNK inhibitor peptide (JNKi) were purchased from Biomol (Plymouth Meeting, PA). All reagents were prepared in either sterile phosphate-buffered saline (PBS) or DMSO, except NAC, which was dissolved in media and the pH adjusted to 7.4 prior to use.

Cell culture and treatments

The murine TAMH hepatocyte cell line is an immortalized, transformed cell line derived from hepatocytes isolated from a TGF-α transgenic mouse and retains a well-differentiated hepatocytic phenotype [42]. TAMH cells were maintained in serum-free DMEM/F12 medium (Life Technologies, Grand Island, NY) supplemented with 5 μg/ml insulin, 5 μg/ml transferrin, 5 ng/ml selenium (ITS premix, Collaborative Biomedical Products, Bedford, MA), 10 mM nicotinamide, 0.1 μM dexamethasone, and 50 μg/ml gentamicin. Mouse embryo fibroblast (MEF) cell lines derived from wild-type mice and mice lacking Nrf1 or Nrf2 have been described elsewhere [43,44]. MEF cells were maintained in DMEM medium supplemented with 15% fetal bovine serum, 1% penicillin/streptomycin, 2 mM glutamine, 0.1 mM non-essential amino acids and 150 μM β-mercaptoethanol. Cells were cultured at 37°C in a humidified 6% CO_2 atmosphere and all experiments were performed at 90–100% confluency. In some experiments, cells were preincubated with various agents for 1 h prior to treatment with As3+. For mRNA half-life studies, cells were cotreated with 500 ng/ml ActD and 10 μM As3+.

RNA analysis

Cells were seeded at a density of 5×10^6 in 100 mm plates. Total RNA was isolated from cells utilizing the RNeasy Mini Kit (Qiagen Inc., Santa Clarita, CA). For Northern blot analysis, RNA (10–20 μg) was resolved on formaldehyde gels and transferred to GeneScreen Plus membranes (Dupont-New England Nuclear, Boston, MA). GCLC, GCLM, and GAPDH cDNA probes were generated as previously described [45] and radiolabeled with [α-^{32}P]dCTP (3000 Ci/mmol; NEN) using the Random Prime Kit (Roche Molecular Biochemicals, Indianapolis, IN). Relative levels of *Gclc*, *Gclm*, and *Gapdh* mRNA were determined using a Storm Phosphoimager (Molecular Dynamics, Sunnyvale, CA). Relative *Gclc* and *Gclm* mRNA levels were normalized to *Gapdh* and presented as fold increase over untreated control. For real-time RT-PCR, total RNA (2 ug) was subjected to reverse transcription followed by real-time quantitative PCR for *Gclc* and *β-Actin* as previously described [46]. Relative *Gclc* mRNA levels were normalized to *β-Actin* and presented as fold increase over untreated control.

Nuclear run-on analysis

Cells from 150 mm plates (~1×10^7 cells) were washed once with ice-cold Solution I (10 mM Tris, pH 7.4, 150 mM KCl, 4 mM MgOAc), and then incubated in Solution I at 4°C for 5 min. Cells were then scraped and pelleted at 300 × g. Cells were lysed by gentle vortexing in Solution II (Solution I + 0.5% Nonidet P-40) for 10 min on ice. Nuclei were pelleted for 10 min at 500 × *g* through a 0.6 M sucrose gradient, resuspended in 100 mu;L of Solution III (40% glycerol, 50 mM $MgCl_2$, 0.1 mM EDTA) and stored in liquid nitrogen. Thawed nuclei were mixed with 45 μL of reaction buffer (1 mM each of ATP, GTP, CTP, 100 μCi of [α-^{32}P]UTP (3000 Ci/mmol; NEN) and incubated at 30°C for 30 min with shaking. The reaction was stopped by the addition of 800 μL of TRIzol (Life Technologies Inc., Carlsbad, CA) and RNA was isolated according to the manufacturer's protocol. Purified ^{32}P-labeled RNA was hybridized to Hybond nylon membrane (Amersham Biosciences, Piscataway, NJ) containing 5 μg of linearized *Gclm*, *Gclc*, and *β-Actin* cDNA. Membranes were hybridized at 42°C for 24 h and then washed in 2X SSC at 42°C for 30 min and in 2X SSC/0.5% SDS at 42°C for 30 min. Band densities were quantitated using a Storm Phosphoimager and the relative levels of *Gclc* and *Gclm* were normalized to *β-Actin*. The normalized levels of *Gclc* and *Gclm* transcribed *in vitro*, which are proportional to relative transcriptional rates, were compared independently and presented as fold increase over their respective untreated control values.

Western blot analysis and JNK assay

Cells were seeded at a density of 2×10^6 in 60 mm plates. Cells were lysed by either a brief sonication on ice in TES/SB buffer as described previously [47], or incubated on ice with TX lysis buffer (20 mM HEPES pH 7.4, 2 mM ETDA, 50 mM β-glycerolphosphate, 1 mM sodium orthovanadate, 10% glycerol, 1% Triton X-100, 1X protease inhibitors). Lysates were clarified by centrifugation and equal amounts of soluble protein (20–25 μg) were resolved on 10% or 12% SDS-polyacrylamide gels and transferred to PVDF membranes (Millipore, Bedford, MA). For analysis of GCL holoenzyme formation whole cell extracts were prepared in the absence of reducing equivalents and were resolved on native 10% PAGE gels in the absence of SDS. Samples for these studies were not boiled prior to gel loading and the gels were resolved in Tris/Glycine buffer at 4°C prior to transfer to PVDF membranes. Membranes were blocked in Tris-buffered saline/0.1% Tween-20 (TBST) containing 5% non-fat milk, prior to incubation with primary antibody in TBST containing 0.5% milk. Membranes were probed for GCLC, GCLM [45,47], βActin (Sigma), JNK, p38 MAPK, ERK2 (Santa Cruz Biotechnology, Santa Cruz, CA), phospho-p38 MAPK, phospho-JNK and phospho-Erk (Cell Signaling, Beverly, MA). Anti-mouse-HRP and anti-rabbit HRP secondary antibodies (Amersham Biosciences) were used at 1:5000 in TBST containing 0.5% milk. The immunocomplex was visualized by chemoluminescence (Dupont-New England Nuclear, Boston, MA) and quantitated using NIH image 6.1 (NIH, Rockville Pike Bethesda, MD). The immunoreactive bands shown in Figures 9D and 9F were identified as monomeric GCLC and/or GCL holoenzyme based on their co-migration with recombinant murine GCLC and GCL holoenzyme protein [48]. JNK activity was measured as previously described [49].

Glutathione and GCL activity assays

Total glutathione content (GSH + GSSG) was determined by a modification of the Tietze assay [47]. Cell extracts were prepared as previously described [45,47] and GSH levels were determined against a standard curve of GSSG and levels calculated per μg of soluble protein in the original cell extract. This value was utilized to determine the relative change in intracellular GSH levels compared to untreated samples. GCL specific activity was determined as described previously [45].

Statistical analysis

Data are presented as averages +/− SEM of at least three experiments. Statistical analysis was performed using GraphPad Prism 4 (GraphPad Software, San Diego, CA). Results were compared by two-tailed *t*-test or one-way ANOVA with Tukey's post test where appropriate. Mean differences were considered significant when $p < 0.05$.

RESULTS

Coordinate induction of *Gclc* and *Gclm* gene expression following As3+ treatment in murine TAMH hepatocyte cells

As3+ up-regulates several enzymes associated with the GSH antioxidant defense system in various cell types [29,31]. To determine whether As3+ induced *Gcl* subunit expression in hepatocytes, TAMH murine hepatocytes were treated with As3+ and steady-state mRNA levels of *Gclc* and *Gclm* were analyzed by northern blotting. Treatment of TAMH cells with 10 μM As3+ resulted in the time-dependent coordinate induction of both *Gclc* and *Gclm* (Fig. 1A). As3+ caused a transient induction in *Gclc* gene expression with maximum expression occurring within 4 h of treatment (~4-fold). In contrast, As3+-induced *Gclm* expression was more prolonged, with maximal expression occurring within 4 h (~4-fold). Induction of *Gclc* and *Gclm* by As3+ was also dose-dependent (Fig 1B). As3+ concentrations as low as 1–2 μM

resulted in a 1.5–2-fold increase in *Gclc* and *Gclm* mRNA levels, while maximal induction of both subunits (3–4-fold) was observed at As3+ concentrations above 10 μM.

As3+ increases the rate of *Gclc* and *Gclm* transcription

Both transcriptional and post-transcriptional mechanisms have been reported to contribute to increased steady-state levels of *Gclc* and *Gclm* mRNA [28,50–54]. Nuclear run-on analyses were performed to determine whether As3+ increased the rate of transcription of the *Gclc* and/or *Gclm* genes. As3+ induced a time-dependent increase in the transcription rates of both *Gclc* and *Gclm* (Fig. 2). As3+ increased *Gclm* and *Gclc* transcription ~2-fold and ~3-fold, respectively, suggesting that enhanced transcription contributes to the increased steady-state *Gclc* and *Gclm* mRNA levels in As3+-treated TAMH cells.

Differential post-transcriptional regulation of *Gclc* and *Gclm* mRNA stability by As3+

While As3+ increased the rate of *Gclc* and *Gclm* transcription, post-transcriptional effects on mRNA stability can also influence steady-state *Gclc* and *Gclm* mRNA levels [50–53]. To examine this possibility, we determined whether As3+ altered the half-life of *Gclc* and/or *Gclm* mRNA. TAMH cells were incubated with actinomycin D (500 ng/ml) in the absence or presence of As3+ (10 μM) and the time-dependent decay of *Gclc* and *Gclm* mRNA levels analyzed by Northern blotting (Fig. 3). In untreated cells, the half-lifes of the murine *Gclc* and *Gclm* mRNAs were ~4 h and ~8 h, which is consistent with previously published values [50, 52,53]. While treatment with As3+ had little effect on the half-life of *Gclc* mRNA, As3+ dramatically increased the half-life of *Gclm* mRNA (~3-fold). These findings suggest that As3+-induced *Gclc* expression is the result of increased transcription, while elevated *Gclm* levels are mediated by both increased gene transcription and post-transcriptional stabilization of the *Gclm* mRNA transcript. Thus, while As3+ coordinately induces both *Gcl* subunits, these responses are mediated by quite distinct molecular mechanisms.

de novo protein synthesis is required for As3+-induced *Gclc* and *Gclm* expression

While transcriptional and post-transcriptional mechanisms are involved in As3+-induced *Gclc* and/or *Gclm* expression, it is unclear whether these effects are primary or secondary responses requiring *de novo* protein synthesis. To determine whether As3+-induced *Gcl* subunit expression was dependent on *de novo* protein synthesis, As3+-induced *Gclc* and *Gclm* expression were analyzed in the presence of the protein synthesis inhibitor cycloheximide (CHX). As shown in Figure 4, CHX abolished As3+-induced expression of both *Gclc* and *Gclm*. In contrast to previous studies conducted in glioma cells [52], CHX alone had no effect on steady-state *Gclc* or *Gclm* mRNA levels at any time point analyzed (up to 8 h; data not shown). Thus, while there are contradictory reports concerning the involvement of *de novo* protein synthesis in regulating the inducible expression of *Gclc* and *Gclm* [50,52,55–57], these findings suggest that a newly synthesized protein(s) is necessary for As3+ induction of *Gclc* and *Gclm* in the TAMH cell model.

Differential sensitivity of As3+-induced *Gclc* and *Gclm* expression to N-acetylcysteine

Many As3+-induced transcriptional responses are thought to be mediated by increased production of ROS [12,58–60], which can activate transcription mediated by ARE, AP1 and NF-kB promoter elements [28]. To determine whether As3+-induced *Gclc* and *Gclm* expression was redox sensitive, we utilized the antioxidant and GSH pro-drug N-acetylcysteine (NAC). Treatment of TAMH cells with 10 mM NAC for 1 h resulted in a ~5-fold increase in intracellular GSH levels (data not shown). Cells were preincubated with NAC and the time-dependent induction of *Gclc* and *Gclm* expression in response to As3+ was assessed by northern blotting. NAC pretreatment abolished As3+-induced *Gclc* expression, while slightly attenuating As3+-induced *Gclm* expression (~30%) (Fig. 5). These findings suggest that while

As3+-induced *Gclc* expression is highly sensitive to intracellular GSH levels, induction of *Gclm* is only partially regulated by alterations in cellular thiol redox homeostasis. This differential sensitivity to intracellular GSH levels provide further evidence that distinct molecular mechanisms mediate As3+-induced *Gclc* and *Gclm* expression.

As3+ induces *Gclc* and *Gclm* expression independent of Nrf1 or Nrf2

The Cap-n-collar bZIP transcription factors Nrf1 and Nrf2 contribute to the basal and inducible expression of *Gclc* and *Gclm* [43,44,61–65]. Furthermore, As3+ has been shown to increase Nrf2 expression in multiple cell types [9,30,41,66,67]. To directly assess the putative role of Nrf1/2 in As3+-induced *Gclc* and *Gclm* expression we utilized mouse embryo fibroblasts (MEF) isolated from wild-type (WT), Nrf1−/− and Nrf2−/− mice [43,44]. As shown in Figure 6A, As3+ treatment resulted in a similar profile of *Gclc* and *Gclm* induction in WT MEFs as observed in TAMH cells (see Fig. 1). As3+ caused a transient 3–4-fold increase in *Gclc* expression (maximal at 4 h), and a more prolonged 6–7-fold increase in *Gclm* expression (maximal at 8 h) in the WT MEF cell line. Surprisingly, As3+-induced *Gclc* and *Gclm* expression was not dramatically different in the WT, Nrf1−/−, or Nrf2−/− MEF cell lines. There was little difference in either the time course or fold-increase in As3+-induced *Gclm* expression in any of these cell lines. As3+-induced *Gclc* expression was also similar in the WT and Nrf1−/− MEF cell lines. While there was an attenuation and delay in As3+-induced *Gclc* expression in the Nrf2−/− MEF cell line, As3+ treatment still increased steady-state *Gclc* mRNA levels ~3-fold. As a positive control for Nrf-dependent transcription, *tert*-butylhydroquinone (tBHQ)-inducible expression of *Gclc* and *Gclm* was examined. tBHQ is the major metabolite of the phenolic antioxidant butylated hydroxyanisole (BHA) and Nrf2 is required for both BHA-induced *Gclc* expression *in vivo* [62] and tBHQ-induced *Gclc* and *Gclm* expression in MEF cells [65]. Consistent with previous studies [65], tBHQ treatment resulted in the time-dependent induction of both *Gclc* and *Gclm* in WT MEFs (Fig. 6B). Importantly, while tBHQ induction of both subunits in the Nrf1−/− MEFs was attenuated, tBHQ-induced *Gclc* and *Gclm* expression was abolished in the Nrf2−/− MEF cell line. These findings suggest that while Nrf2 is required for tBHQ-induced *Gclc/Gclm* expression, As3+-induced *Gclc/Gclm* expression occurs independent of Nrf1 and Nrf2.

The role of MAPKs in As3+-induced *Gclc* and *Gclm* expression

As3+ activates multiple MAPK pathways that have been implicated in the inducible expression of *Gclc* and *Gclm* [37–40]. In light of our demonstration that As3+-induced *Gclc* and *Gclm* expression was Nrf1/2-independent, we examined the putative role of the MAPK pathways in As3+-induced *Gclc* and/or *Gclm* expression in the TAMH cell model. To identify the MAPK pathways activated by As3+ in this cell model, TAMH cells were treated with various concentrations of As3+ for 4 h and MAPK activation assessed by immunoblot analysis utilizing phospho-specific antibodies that recognize the activated forms of JNK, p38 MAPK and ERK. As3+ treatment resulted in the dose-dependent activation of JNK, p38 MAPK and ERK (Figure 7). In the case of JNK, As3+-induced kinase activity (data not shown) correlated well with the appearance of phosphorylated JNK. Importantly, As3+ activated all three MAPK pathways at an As3+ concentration (10 uM) employed for all other experiments performed in these studies. To directly examine the involvement of these signal transduction pathways in As3+-induced *Gclc/Gclm* expression, we employed pharmacological inhibitors of the JNK (SP600125), p38 MAPK (SB202190) and ERK (PD98059) pathways. Cells were pretreated with these inhibitors and As3+-induced *Gclc* and *Gclm* expression was analyzed (Fig. 8A and 8B). Inhibition of the ERK pathway utilizing the MEK1/2 inhibitor PD98059 slightly attenuated As3+-induced *Gclc* expression (~20% reduction), but had no effect on As3+-induced *Gclm* expression. In contrast, the p38 MAPK inhibitor SB202190 reduced As3+-induced *Gclc* and *Gclm* expression by ~50% and ~30%, respectively. The JNK inhibitor SP600125 had little effect on As3+-induced *Gclm* expression. Surprisingly, SP600125 dramatically enhanced As3+-induced

Gclc gene expression, increasing steady-state *Gclc* levels ~2-fold over that observed in response to As3+ alone. Given the potential for non-specific effects of SP600125 [54,68], a more selective peptide JNK inhibitor (JNKi) was employed in conjunction with real-time RT-PCR to confirm the role of JNK in mediating this response. Consistent with the Northern blot findings, SP600125 was found to significantly potentiate As3+-induced *Gclc* expression (Fig 8C). However, JNKi had no effect on As3+-induced *Gclc* expression (Fig. 8C). These findings suggest that JNK is not involved in As3+-induced *Gclc* expression and does not mediate the superinduction of *Gclc* observed in the presence of SP600125. None of these inhibitors had a marked effect on basal levels of *Gclm* mRNA (<25% reduction), while SB202190 and PD98059 reduced basal *Gclc* mRNA levels by 40–50% (data not shown). Importantly, SP600125 had little effect on basal *Gclc* mRNA levels (data not shown), indicating that while SP600125 enhanced As3+-induced *Gclc* mRNA levels, it did not affect constitutive *Gclc* expression.

As As3+ activated all three MAPK pathways, the potential additive effects of these protein kinase pathways on As3+-induced *Gclc* and *Gclm* expression was examined by assessing the combinatorial effects of the inhibitors described above (Fig. 8A and 8B). Various combinations of inhibitors had no greater effect on As3+-induced *Gclm* expression than the p38 MAPK inhibitor SB202190 alone (~30% inhibition). Analysis of *Gclc* mRNA levels indicated that the inhibitory effects of PD98059 and SB202190 on As3+-induced *Gclc* expression were additive, reducing *Gclc* levels to that observed in untreated cells. Interestingly, cotreatment with SB202190 abolished SP600125-induced potentiation of As3+-induced *Gclc* expression, resulting in reduced *Gclc* levels similar to that observed in cells pretreated with SB202190 alone. In contrast, cotreatment with PD98059 had no effect on the ability of SP600125 to enhance As3+-induced *Gclc* expression. In aggregate, these findings suggest that As3+ induction of *Gclm* is partially mediated by the p38 MAPK pathway, while both the p38 MAPK and ERK pathways contribute to As3+-induced *Gclc* expression.

As3+ increases GCLC and GCLM protein expression and GCL holoenzyme formation and enzymatic activity

While As3+ increased the steady-state mRNA levels of both *Gcl* subunits in TAMH cells, it was of interest to determine whether these transcriptional responses were functionally relevant. To determine whether As3+ treatment increased GCL subunit protein expression, GCLC and GCLM protein levels were examined by immunoblotting (Fig. 9A). As3+ treatment resulted in a time-dependent increase in the expression of both GCLC and GCLM. GCLC levels were increased ~2-fold after 16–24 h of As3+ treatment when normalized to βActin levels (Fig. 9B, open circles). As3+ caused an even greater increase in GCLM protein expression with a 3–4-fold induction observed after 16–24 h of treatment (Fig. 9A and 9B, closed circles). These increases in GCLC and GCLM protein levels correlated with increased GSH biosynthetic capacity as exposure to As3+ for 16 h resulted in a 2-fold increase in GCL activity (Fig. 9C). To determine whether As3+ treatment increased GCL activity by enhancing GCL holoenzyme formation, whole cell extracts were resolved by native gel electrophoresis and GCL holoenzyme detected by immunoblotting for GCLC and GCLM (Fig. 9D). Immunoblotting for GCLC revealed two immunoreactive bands of differing electrophoretic mobility (Fig. 9D, upper panel). The identity of these bands was established by their comigration with purified recombinant GCLC protein and GCL holoenzyme ([48], data now shown). The identity of the GCL holoenzyme band was also confirmed by the presence of GCLM (Fig. 9D, lower panel). Importantly, treatment with As3+ resulted in an increase in GCL holoenzyme formation detected with either α-GCLC or α-GCLM antisera, which was associated with a concomitant decrease in monomeric GCLC. Increased GCL holoenzyme formation and activity could result from either *de novo* synthesis of the GCL subunits or post-translational control of pre-existing GCL protein [27,28]. To determine whether increased GCL subunit protein expression *per*

se was required for As3+-induced GCL holoenzyme formation and activity, cells were pretreated with the protein synthesis inhibitor cycloheximide (CHX). As shown in Fig. 9E and 9F, pretreatment with CHX abolished As3+-induced GCL activity and GCL holoenzyme formation, respectively. CHX alone had no effect on basal GCL activity (data not shown). In aggregate, these findings are consistent with a model in which As3+-induced GCL activity is mediated by the induction of *Gclc* and *Gclm* gene expression, increased GCL subunit protein expression and increased GCL holoenzyme formation.

Discussion

Chronic exposure to low levels of As3+ induces transformation *in vitro*, while acute exposure to high concentrations induces apoptotic cell death [21]. Interestingly, As3+-transformed cells often exhibit increased resistance to As3+-induced apoptosis and the GSH antioxidant defense system may play a central role in the development of this resistant phenotype. While both acute and chronic As3+ exposure induce an adaptive up-regulation of the GSH antioxidant system, the molecular mechanism(s) mediating these responses are not known. In this study, we have identified distinct transcriptional and post-transcriptional mechanisms and signal transduction pathways that mediate As3+-induced expression of the subunits of GCL, the rate-limiting enzyme in GSH biosynthesis.

As3+ has been reported to induce *Gclc* gene expression in human keratinocytes [9,29,30] and rat lung epithelial cells [31]. Our findings confirm and extend these studies by demonstrating that As3+ coordinately induces both *Gclc* and *Gclm* gene expression in the TAMH murine hepatocyte cell line, albeit by quite distinct mechanisms. Transcriptional and post-transcriptional mechanisms contribute to the steady-state levels of *Gclc* and *Gclm* mRNA in response to various oxidative stressors [24,28,32,54]. While As3+ increased the rate of transcription of both *Gclc* and *Gclm*, As3+ only enhanced the post-transcriptional stabilization of *Gclm* mRNA in TAMH cells. These findings are in contrast to the post-transcriptional stabilization of both *Gclc* and *Gclm* mRNA in response to 4-hydroxynonenal (4-HNE) or diethylmaleate (DEM) [50,53]. As3+-induced *Gclm* gene transcription and enhanced *Gclm* mRNA stability, together with the longer $t_{1/2}$ of *Gclm* mRNA compared to *Gclc* mRNA, likely contribute to the more prolonged increase in steady-state levels of *Gclm* mRNA relative to *Gclc* mRNA. While the relative translational efficiency of the *Gclc* and *Gclm* mRNAs is not known, this may provide the molecular basis for the greater increase in GCLM protein (4-fold) versus GCLC protein (2-fold) in response to As3+ treatment. As3+ also induced *Gcl* subunit gene expression in a similar dose-dependent manner. Importantly, while maximal induction occurred at slightly toxic concentrations of As3+ (>10 uM), both subunits were induced at toxicologically and physiologically relevant As3+ concentrations (1–2 uM) in the TAMH cell model.

As3+-induced *Gclc* and *Gclm* expression were both dependent on *de novo* protein synthesis. In contrast, inhibition of *de novo* protein synthesis selectively prevents 4-HNE-induced *Gclm* expression and menadione-induced *Gclc* expression, in rat [50] and human [56] lung epithelial cells, respectively, while having no effect on *Gclc* or *Gclm* gene induction in response to ACNU or cigarette smoke condensate [52,55]. There are also conflicting reports of the involvement of *de novo* protein synthesis in constitutive *Gclc* and *Gclm* expression. Cycloheximide alone had no effect on basal *Gclc* expression in our cell model, which is consistent with previous reports in HepG2 cells [69] and human bronchial epithelial cells [56], but in contrast to findings in human glioma cells [52]. These findings highlight the differential involvement of *de novo* protein synthesis in mediating the constitutive and inducible expression of the *Gcl* subunits in response to As3+ and other types of oxidative stress in various cell types.

Similar to the human *Gclc* and *Gclm* gene promoters [33], the proximal region of the murine *Gclc* and *Gclm* promoters contain numerous *cis*-elements that could potentially mediate As3+-inducibility, including ARE, AP1, MTF-1 and NF-kB sites [70–72]. Nrf1 and Nrf2 play important roles in ARE-mediated gene transcription and the constitutive and inducible expression of multiple phase II enzymes, including *Gclm* and *Gclc* [28,32–34,73,74]. However, Nrf1 and Nrf2 are distinct in their ability to modulate *Gcl* subunit gene expression [43,44, 63]. While paraquat- and DEM-inducible *Gclm* expression is suppressed in Nrf1-deficient MEFs [43,63], deletion of Nrf1 had no effect on As3+- or tBHQ-induced *Gclc* and *Gclm* mRNA expression. In contrast, tBHQ-induced *Gclc* and *Gclm* mRNA expression was abolished in Nrf2-deficient MEFs, which is consistent with previous studies [65]. Surprisingly, deletion of Nrf2 had little effect on As3+-induced *Gclm* and *Gclc* expression. The only notable effect was an attenuation and delay in As3+-induced *Gclc* expression in Nrf2-deficient MEFs. *In vitro* studies indicate that Nrf1/2-dependent *Gcl* subunit expression is at least partially mediated by antioxidant response elements (ARE) in the *Gclc* and *Gclm* promoters [28,33,54]. However, while the murine *Gclc* and *Gclm* promoters contain functional ARE sites [70–72] and As3+ increases Nrf2 protein expression and ARE-mediated gene transcription [22,30,66,67,75], Nrf2 is not required for As3+-induced *Gclc* and *Gclm* gene transcription. In contrast, Nrf2 is required for *Gclc* induction in response to tBHQ ([65] and Fig. 6), DEM [63], and indomethacin [76, 77]. Such findings do not exclude the possibility that Nrf1 and Nrf2 exhibit stimulus-dependent functional redundancy and can compensate for each other in As3+-induced, but not tBHQ-induced *Gcl* subunit expression. Interestingly, while Nrf1/2 mediate tBHQ-induced rat *Gclc* expression this occurs via AP-1 and NF-kB binding sites and not ARE sites, which are not present in the rat promoter [65,78,79]. Nrf2 also plays an essential role in mediating As3+-induced transcription of certain target genes. For instance, As3+-induced NAD(P)H:quinone oxidoreductase I (NQO1), and heme oxygenase-1 (HO-1) and MSP23 (peroxiredoxin 1) expression is attenuated or abolished in Nrf2-deficient MEFs [66,80] and macrophages [81], respectively. A dominant-negative Nrf2 mutant also inhibited As3+-induced ARE-mediated transcriptional activity [75] and HO-1 expression in L929 fibroblasts [82] and HepG2 hepatoma cells [83]. Cell type-specific differences have also been reported in the constitutive and inducible expression of *Gclc* and *Gclm* [84]. In aggregate, these findings suggest that while As3+-induced expression of some phase II enzymes are Nrf2-dependent in certain cell types, Nrf2 is not required for As3+-induced *Gclc* or *Gclm* gene expression in murine hepatocytes even though the murine promoters of both subunits contain functional ARE binding sites [70–72].

Multiple MAP kinase pathways have also been implicated in oxidative stress-induced *Gcl* subunit expression [37–40]. In TAMH cells, As3+ treatment induced the dose-dependent activation of JNK, p38 MAPK, and ERK and pharmacological inhibitors of these pathways were employed to determine their involvement in As3+-induced *Gclc* and *Gclm* gene expression. While inhibition of the p38 MAPK or ERK pathway alone partially suppressed As3+-induced *Gclc* expression, inhibition of both pathways was required to abolish *Gclc* induction. These findings are analogous to the involvement of both p38 MAPK and ERK in PDTC-induced *Gclc* expression in HepG2 cells [40,85], while ERK activation alone appears to be required for 4-HNE-induced *Gclc* expression in rat L2 alveolar epithelial cells [37,39, 54]. Interestingly, the JNK inhibitor SP600125 dramatically potentiated As3+-induced *Gclc* expression. However, SP600125 is known to inhibit a number of protein kinases with similar efficacies that could potentially mediate this response [68]. Importantly, the inability of the highly specific peptide JNK inhibitor JNKi to elicit a similar superinduction of *Gclc* expression indicates that the SP600125 effects are not mediated by JNK inhibition. These findings also suggest that JNK is not involved in As3+-induced *Gclc* gene expression, which contrasts with previous reports that JNK activation is required for 4-HNE- and glucose-deprivation-induced *Gclc* expression in HBE1 human bronchial epithelial cells [37] and MCF7 cells [38], respectively. While the cellular and molecular basis for these disparities are not known, there

appear to be distinct stimuli-, cell type-, concentration-, and species-dependent differences in the mechanisms regulating both the constitutive and inducible expression of the *Gclc* and *Gclm* genes [37,39,40,54,84].

While the transcriptional effects of SP600125 appear to be JNK-independent, SP600125 clearly potentiated As3+-induced *Gclc* expression in the TAMH murine hepatocyte cell line. This response was subunit specific as SP600125 had no effect on As3+-induced *Gclm* expression. SP600125 also had no effect on basal *Gclc* gene expression, suggesting that this superinduction resulted from inhibition of an As3+-activated signal transduction pathway. While the molecular target mediating this SP600125 response is not known, these findings imply that As3+ is activating an SP600125-sensitive protein kinase that is suppressing *Gclc* expression in the TAMH cell model. This is reminiscent of p38 MAPK-mediated suppression of ARE-mediated gene transcription and induction of phase II enzymes in human HepG2 and murine Hepa1C1C7 hepatoma cell lines [86]. However, the ability of the p38 MAPK inhibitor SB203580 to abolish SP600125-mediated potentiation of As3+-induced *Gclc* expression suggests that this response is mediated by activation of the p38 MAPK pathway, which we have shown contributes to As3+-induced *Gclc* expression (Fig. 8). Interestingly, SP600125 rapidly stimulates p38 MAPK phosphorylation and activity in the MIN6 mouse pancreatic cell line [87]. Additional studies are required to reveal the molecular mechanisms and putative involvement of p38 MAPK in SP600125-mediated potentiation of As3+-induced *Gclc* expression.

In contrast to As3+-induced *Gclc* expression, p38 MAPK is the only MAPK involved in As3+-induced *Gclm* expression and it only accounts for ~30% of steady-state *Gclm* mRNA levels, suggesting the involvement of additional signaling pathways. Furthermore, the effects of p38 MAPK could result from either enhanced *Gclm* mRNA stabilization or activation of *Gclm* gene transcription, both of which contribute to steady-state *Gclm* mRNA levels. In fact, p38 MAPK has been implicated in both As3+-induced gene transcription and post-transcriptional stabilization of various mRNA species [88]. While our findings indicate that As3+ did not increase steady-state murine *Gclc* mRNA levels via mRNA stabilization, Song et al. have shown that p38 MAPK activation enhances human *Gclc* mRNA stability in response to several prooxidants, including tBHQ and menadione [51]. An AUUUA HuR recognition sequence in the 3′-UTR of human *Gclc* was found to be responsible for HuR-mediated regulation of *Gclc* mRNA stability [51]. It remains to be determined whether the 3′-UTR of murine *Gclc* and/or human or murine *Gclm* contain functional AU-rich sequences capable of binding mRNA stabilizing factors such as HuR.

NAC-mediated inhibition of As3+-induced *Gclc* induction and attenuation of *Gclm* induction suggests that redox-sensitive mechanisms are involved in the induction of both subunits. Furthermore, the ability of NAC to only partially suppress As3+-induced *Gclm* expression (~30–50%) is consistent with the selective inhibition of either gene transcription or post-transcriptional *Gclm* mRNA stabilization. Interestingly, the relative level of NAC-mediated inhibition of As3+-induced *Gclm* expression correlated quantitatively with the inhibition by the p38 MAPK inhibitor SB203580 (Fig. 7; 30–40%). Given that NAC abolished As3+-induced p38 MAPK, JNK, and ERK in TAMH cells (data not shown) it is intriguing to speculate that the partial suppression of As3+-induced *Gclm* expression is due to NAC-mediated inhibition of p38 MAPK activity. Correspondingly, NAC-mediated inhibition of As3+-induced *Gclc* expression could result from inhibition of As3+-induced activation of p38 MAPK and ERK.

While transcriptional induction of the *Gcl* subunit mRNAs invariably leads to increased GCL protein translation, it was important to demonstrate functionality with regard to GCL enzymatic activity. As expected, As3+-induced *Gcl* subunit gene expression correlated with increased

GCL subunit protein expression and GCL enzymatic activity. Direct quantitation and functional studies indicate that GCLM is limiting for GCL holoenzyme formation and GCL activity both *in vivo* and in cultured cell systems [48,89–91]. While we did not directly measure the molar amounts and ratios of the GCL subunits, analysis of GCL holoenzyme composition by native gel electrophoresis confirmed that GCLM was limiting in TAMH cells. This was based on the presence of both monomeric GCLC and heterodimeric holo-GCL bands upon immunoblotting with α-GCLC antisera and the detection of only a single band comigrating with holo-GCL when immunoblotting with α-GCLM antisera. Importantly, As3+ treatment enhanced GCL holoenzyme formation as judged by the shift of monomeric GCLC protein to heterodimeric GCL holoenzyme and the increased amount of GCLM protein present in the holo-GCL complex (Fig. 8D). The greater relative induction of the GCLM subunit (~4 fold for GCLM vs. ~2-fold for GCLC) and the fact that GCLM is limiting suggest that increased expression of GCLM likely contributes more to As3+-induced GCL enzymatic activity via increased GCL holoenzyme formation than increased GCLC expression *per se*. Preferential induction of the GCLM subunit is also observed in response to 4-HNE in rat lung epithelial cells [39], cysteine deprivation in HepG2 cells and the rat liver *in vivo* [91], oxidized LDL in murine macrophages [71], and thyroid hormone in rat astrocytes [92]. Irrespective of the relative contribution of GCLC or GCLM protein, the inhibitory effects of cycloheximide suggest that As3+-induced GCL holoenzyme formation and activity result from increased *de novo* synthesis of the GCL subunits and not post-translational modification of pre-existing GCL protein.

In aggregate, this study identified multiple molecular mechanisms that contribute to increased GCL subunit expression and activity in response to acute As3+ exposure. While As3+ coordinately induced *Gclc* and *Gclm* gene expression, distinct signal transduction pathways and transcriptional and post-transcriptional regulatory mechanisms mediated these responses. Importantly, these transcriptional events were functionally relevant, leading to increased GCL subunit protein expression, GCL holoenzyme formation, and GCL activity. In light of the importance of intracellular GSH levels in dictating cellular sensitivity to As3+-induced apoptosis, induction of GCL expression and activity is likely a cytoprotective adaptive response to As3+ exposure. In this regard, increased GSH biosynthetic capacity may play a fundamental role in As3+ adaptation and apoptosis evasion during As3+-induced hepatocarcinogenesis and could also have clinical implications with regard to the use of arsenic trioxide as a chemotherapeutic in the treatment of acute promyelocytic leukemia. However, it remains to be determined whether up-regulation of cellular GSH biosynthetic capacity *per se* affects As3+-induced apoptosis and/or transformation.

Acknowledgments

This work was supported by NIH grants CA75316, CA90473, and ES07033 (to CCF), CA23226 and CA74131 (to NF), and ES04696, ES10849, AG01751, and ES07033 (to TJK). James A. Thompson is a Mary Gates Scholar. The authors thank Zahra Afsharinejad for performing the real-time RT-PCR analyses and Donald S. Backos for assistance with statistical analyses.

List of Abbreviations

As3+
: arsenite

GSH
: glutathione

GSSG
: glutathione disulfide

GCL
glutamate-cysteine ligase

GCLC
catalytic subunit of glutamate-cysteine ligase

GCLM
modifier subunit of glutamate-cysteine ligase

GST
glutathione S-transferase

Nrf1/2
NF-E2-related factor 1/2

ROS
reactive oxygen species

NAC
N-acetylcysteine

CHX
cycloheximide

ActD
actinomycin D

BSO
buthionine sulfoximine

tBHQ
tert-butylhydroquinone

4-HNE
4-hydroxynonenal

GAPDH
glyceraldehyde-3-phosphate dehydrogenase

ARE
antioxidant response element

UTR
untranslated region

MEF
mouse embryo fibroblast

References

1. Yoshida T, Yamauchi H, Fan Sun G. Chronic health effects in people exposed to arsenic via the drinking water: dose-response relationships in review. Toxicol Appl Pharmacol 2004;198:243–252. [PubMed: 15276403]
2. Centeno JA, Mullick FG, Martinez L, Page NP, Gibb H, Longfellow D, Thompson C, Ladich ER. Pathology related to chronic arsenic exposure. Environ Health Perspect 2002;110(Suppl 5):883–886. [PubMed: 12426152]
3. Liu J, Waalkes MP. Liver is a target of arsenic carcinogenesis. Toxicol Sci 2008;105(1):24–32. [PubMed: 18566022]

4. Dong Z. The molecular mechanisms of arsenic-induced cell transformation and apoptosis. Environ Health Perspect 2002;110(Suppl 5):757–759. [PubMed: 12426127]
5. Zhao CQ, Young MR, Diwan BA, Coogan TP, Waalkes MP. Association of arsenic-induced malignant transformation with DNA hypomethylation and aberrant gene expression. Proc Natl Acad Sci U S A 1997;94:10907–10912. [PubMed: 9380733]
6. Sens DA, Park S, Gurel V, Sens MA, Garrett SH, Somji S. Inorganic cadmium- and arsenite-induced malignant transformation of human bladder urothelial cells. Toxicol Sci 2004;79:56–63. [PubMed: 14976345]
7. Achanzar WE, Brambila EM, Diwan BA, Webber MM, Waalkes MP. Inorganic arsenite-induced malignant transformation of human prostate epithelial cells. J Natl Cancer Inst 2002;94:1888–1891. [PubMed: 12488483]
8. Chien CW, Chiang MC, Ho IC, Lee TC. Association of chromosomal alterations with arsenite-induced tumorigenicity of human HaCaT keratinocytes in nude mice. Environ Health Perspect 2004;112:1704–1710. [PubMed: 15579417]
9. Pi J, Diwan BA, Sun Y, Liu J, Qu W, He Y, Styblo M, Waalkes MP. Arsenic-induced malignant transformation of human keratinocytes: Involvement of Nrf2. Free Radic Biol Med 2008;45:651–658. [PubMed: 18572023]
10. Huang C, Ma WY, Li J, Goranson A, Dong Z. Requirement of Erk, but not JNK, for arsenite-induced cell transformation. J Biol Chem 1999;274:14595–14601. [PubMed: 10329651]
11. Miller WH Jr, Schipper HM, Lee JS, Singer J, Waxman S. Mechanisms of action of arsenic trioxide. Cancer Res 2002;62:3893–3903. [PubMed: 12124315]
12. Liu SX, Athar M, Lippai I, Waldren C, Hei TK. Induction of oxyradicals by arsenic: implication for mechanism of genotoxicity. Proc Natl Acad Sci U S A 2001;98:1643–1648. [PubMed: 11172004]
13. Kitchin KT, Ahmad S. Oxidative stress as a possible mode of action for arsenic carcinogenesis. Toxicol Lett 2003;137:3–13. [PubMed: 12505428]
14. Romach EH, Zhao CQ, Del Razo LM, Cebrian ME, Waalkes MP. Studies on the mechanisms of arsenic-induced self tolerance developed in liver epithelial cells through continuous low-level arsenite exposure. Toxicol Sci 2000;54:500–508. [PubMed: 10774833]
15. Brambila EM, Achanzar WE, Qu W, Webber MM, Waalkes MP. Chronic arsenic-exposed human prostate epithelial cells exhibit stable arsenic tolerance: mechanistic implications of altered cellular glutathione and glutathione S-transferase. Toxicol Appl Pharmacol 2002;183:99–107. [PubMed: 12387749]
16. Qu W, Bortner CD, Sakurai T, Hobson MJ, Waalkes MP. Acquisition of apoptotic resistance in arsenic-induced malignant transformation: role of the JNK signal transduction pathway. Carcinogenesis 2002;23:151–159. [PubMed: 11756236]
17. Somji S, Zhou XD, Garrett SH, Sens MA, Sens DA. Urothelial cells malignantly transformed by exposure to cadmium (Cd(+2)) and arsenite (As(+3)) have increased resistance to Cd(+2) and As (+3)-induced cell death. Toxicol Sci 2006;94:293–301. [PubMed: 16980690]
18. Pi J, He Y, Bortner C, Huang J, Liu J, Zhou T, Qu W, North SL, Kasprzak KS, Diwan BA, Chignell CF, Waalkes MP. Low level, long-term inorganic arsenite exposure causes generalized resistance to apoptosis in cultured human keratinocytes: potential role in skin co-carcinogenesis. Int J Cancer 2005;116:20–26. [PubMed: 15756686]
19. Coppin JF, Qu W, Waalkes MP. Interplay between cellular methyl metabolism and adaptive efflux during oncogenic transformation from chronic arsenic exposure in human cells. J Biol Chem. 2008
20. Qu W, Kasprzak KS, Kadiiska M, Liu J, Chen H, Maciag A, Mason RP, Waalkes MP. Mechanisms of arsenic-induced cross-tolerance to nickel cytotoxicity, genotoxicity, and apoptosis in rat liver epithelial cells. Toxicol Sci 2001;63:189–195. [PubMed: 11568362]
21. Bode AM, Dong Z. The paradox of arsenic: molecular mechanisms of cell transformation and chemotherapeutic effects. Crit Rev Oncol Hematol 2002;42:5–24. [PubMed: 11923065]
22. Kann S, Estes C, Reichard JF, Huang MY, Sartor MA, Schwemberger S, Chen Y, Dalton TP, Shertzer HG, Xia Y, Puga A. Butylhydroquinone protects cells genetically deficient in glutathione biosynthesis from arsenite-induced apoptosis without significantly changing their prooxidant status. Toxicol Sci. 2005

23. Habib GM, Shi ZZ, Lieberman MW. Glutathione protects cells against arsenite-induced toxicity. Free Radic Biol Med 2007;42:191–201. [PubMed: 17189825]
24. Griffith OW, Mulcahy RT. The enzymes of glutathione synthesis: gamma-glutamylcysteine synthetase. Adv Enzymol Relat Areas Mol Biol 1999;73:209–267. [PubMed: 10218110]
25. Hayes JD, McLellan LI. Glutathione and glutathione-dependent enzymes represent a coordinately regulated defence against oxidative stress. Free Radic Res 1999;31:273–300. [PubMed: 10517533]
26. Ballatori N, Hammond CL, Cunningham JB, Krance SM, Marchan R. Molecular mechanisms of reduced glutathione transport: role of the MRP/CFTR/ABCC and OATP/SLC21A families of membrane proteins. Toxicol Appl Pharmacol 2005;204:238–255. [PubMed: 15845416]
27. Franklin CC, Backos DS, Mohar I, White CC, Forman HJ, Kavanagh TJ. Structure, Function, and Post-Transcriptional Regulation of the Catalytic and Modifier Subunits of Glutamate Cysteine Ligase. Mol Aspects Med. 200810.1016/j.mam.2008.08.009
28. Lu SC. Regulation of glutathione synthesis. Mol Aspects Med. 200810.1016/j.mam.2008.05.005
29. Schuliga M, Chouchane S, Snow ET. Upregulation of glutathione-related genes and enzyme activities in cultured human cells by sublethal concentrations of inorganic arsenic. Toxicol Sci 2002;70:183–192. [PubMed: 12441363]
30. Pi J, Qu W, Reece JM, Kumagai Y, Waalkes MP. Transcription factor Nrf2 activation by inorganic arsenic in cultured keratinocytes: involvement of hydrogen peroxide. Exp Cell Res 2003;290:234–245. [PubMed: 14567983]
31. Li M, Cai JF, Chiu JF. Arsenic induces oxidative stress and activates stress gene expressions in cultured lung epithelial cells. J Cell Biochem 2002;87:29–38. [PubMed: 12210719]
32. Wild AC, Mulcahy RT. Regulation of gamma-glutamylcysteine synthetase subunit gene expression: insights into transcriptional control of antioxidant defenses. Free Radic Res 2000;32:281–301. [PubMed: 10741850]
33. Dickinson DA, Levonen AL, Moellering DR, Arnold EK, Zhang H, Darley-Usmar VM, Forman HJ. Human glutamate cysteine ligase gene regulation through the electrophile response element. Free Radic Biol Med 2004;37:1152–1159. [PubMed: 15451055]
34. Zhang DD. Mechanistic studies of the Nrf2-Keap1 signaling pathway. Drug Metab Rev 2006;38:769–789. [PubMed: 17145701]
35. Nguyen T, Sherratt PJ, Pickett CB. Regulatory mechanisms controlling gene expression mediated by the antioxidant response element. Annu Rev Pharmacol Toxicol 2003;43:233–260. [PubMed: 12359864]
36. Myhrstad MC, Husberg C, Murphy P, Nordstrom O, Blomhoff R, Moskaug JO, Kolsto AB. TCF11/Nrf1 overexpression increases the intracellular glutathione level and can transactivate the gamma-glutamylcysteine synthetase (GCS) heavy subunit promoter. Biochim Biophys Acta 2001;1517:212–219. [PubMed: 11342101]
37. Dickinson DA, Iles KE, Watanabe N, Iwamoto T, Zhang H, Krzywanski DM, Forman HJ. 4-hydroxynonenal induces glutamate cysteine ligase through JNK in HBE1 cells. Free Radic Biol Med 2002;33:974. [PubMed: 12361807]
38. Lee YJ, Galoforo SS, Sim JE, Ridnour LA, Choi J, Forman HJ, Corry PM, Spitz DR. Dominant-negative Jun N-terminal protein kinase (JNK-1) inhibits metabolic oxidative stress during glucose deprivation in a human breast carcinoma cell line. Free Radic Biol Med 2000;28:575–584. [PubMed: 10719239]
39. Liu RM, Borok Z, Forman HJ. 4-Hydroxy-2-nonenal increases gamma-glutamylcysteine synthetase gene expression in alveolar epithelial cells. Am J Respir Cell Mol Biol 2001;24:499–505. [PubMed: 11306445]
40. Zipper LM, Mulcahy RT. Inhibition of ERK and p38 MAP kinases inhibits binding of Nrf2 and induction of GCS genes. Biochem Biophys Res Commun 2000;278:484–492. [PubMed: 11097862]
41. Wang XJ, Sun Z, Chen W, Li Y, Villeneuve NF, Zhang DD. Activation of Nrf2 by arsenite and monomethylarsonous acid is independent of Keap1-C151: enhanced Keap1-Cul3 interaction. Toxicol Appl Pharmacol 2008;230:383–389. [PubMed: 18417180]
42. Wu JC, Merlino G, Cveklova K, Mosinger B, Fausto N. Autonomous growth in serum-free medium and production of hepatocellular carcinomas by differentiated hepatocyte lines that overexpress transforming growth factor alpha 1. Cancer Res 1994;54:5964–5973. [PubMed: 7525051]

43. Kwong M, Kan YW, Chan JY. The CNC basic leucine zipper factor, Nrf1, is essential for cell survival in response to oxidative stress-inducing agents. Role for Nrf1 in gamma-gcs(l) and gss expression in mouse fibroblasts. J Biol Chem 1999;274:37491–37498. [PubMed: 10601325]
44. Chan JY, Kwong M. Impaired expression of glutathione synthetic enzyme genes in mice with targeted deletion of the Nrf2 basic-leucine zipper protein. Biochim Biophys Acta 2000;1517:19–26. [PubMed: 11118612]
45. Franklin CC, Rosenfeld-Franklin ME, White C, Kavanagh TJ, Fausto N. TGFbeta1-induced suppression of glutathione antioxidant defenses in hepatocytes: caspase-dependent posttranslational and caspase-independent transcriptional regulatory mechanisms. Faseb J 2003;17:1535–1537. [PubMed: 12824300]
46. Botta D, Shi S, White CC, Dabrowski MJ, Keener CL, Srinouanprachanh SL, Farin FM, Ware CB, Ladiges WC, Pierce RH, Fausto N, Kavanagh TJ. Acetaminophen-induced liver injury is attenuated in male glutamate-cysteine ligase transgenic mice. J Biol Chem 2006;281:28865–28875. [PubMed: 16840778]
47. Franklin CC, Krejsa CM, Pierce RH, White CC, Fausto N, Kavanagh TJ. Caspase-3-Dependent Cleavage of the Glutamate-L-Cysteine Ligase Catalytic Subunit during Apoptotic Cell Death. Am J Pathol 2002;160:1887–1894. [PubMed: 12000740]
48. Krzywanski DM, Dickinson DA, Iles KE, Wigley AF, Franklin CC, Liu RM, Kavanagh TJ, Forman HJ. Variable regulation of glutamate cysteine ligase subunit proteins affects glutathione biosynthesis in response to oxidative stress. Arch Biochem Biophys 2004;423:116–125. [PubMed: 14871475]
49. Franklin CC, Srikanth S, Kraft AS. Conditional expression of mitogen-activated protein kinase phosphatase- 1, MKP-1, is cytoprotective against UV-induced apoptosis. Proc Natl Acad Sci U S A 1998;95:3014–3019. [PubMed: 9501207]
50. Liu RM, Gao L, Choi J, Forman HJ. γ-glutamylcysteine synthetase: mRNA stabilization and independent subunit transcription by 4-hydroxy-2-nonenal. Am J Physiol 1998;275:L861–869. [PubMed: 9815102]
51. Song IS, Tatebe S, Dai W, Kuo MT. Delayed mechanism for induction of gamma-glutamylcysteine synthetase heavy subunit mRNA stability by oxidative stress involving p38 mitogen-activated protein kinase signaling. J Biol Chem 2005;280:28230–28240. [PubMed: 15946948]
52. Gomi A, Masuzawa T, Ishikawa T, Kuo MT. Posttranscriptional regulation of MRP/GS-X pump and gamma- glutamylcysteine synthetase expression by 1-(4-amino-2-methyl-5- pyrimidinyl) methyl-3-(2-chloroethyl)-3-nitrosourea and by cycloheximide in human glioma cells. Biochem Biophys Res Commun 1997;239:51–56. [PubMed: 9345268]
53. Sekhar KR, Long M, Long J, Xu ZQ, Summar ML, Freeman ML. Alteration of transcriptional and post-transcriptional expression of gamma-glutamylcysteine synthetase by diethyl maleate. Radiat Res 1997;147:592–597. [PubMed: 9146705]
54. Iles KE, Liu RM. Mechanisms of glutamate cysteine ligase (GCL) induction by 4-hydroxynonenal. Free Radic Biol Med 2005;38:547–556. [PubMed: 15683710]
55. Rahman I, Smith CA, Lawson MF, Harrison DJ, MacNee W. Induction of gamma-glutamylcysteine synthetase by cigarette smoke is associated with AP-1 in human alveolar epithelial cells. FEBS Lett 1996;396:21–25. [PubMed: 8906859]
56. Ray S, Watkins DN, Misso NL, Thompson PJ. Oxidant stress induces gamma-glutamylcysteine synthetase and glutathione synthesis in human bronchial epithelial NCI-H292 cells. Clin Exp Allergy 2002;32:571–577. [PubMed: 11972604]
57. Shi MM, Iwamoto T, Forman HJ. gamma-Glutamylcysteine synthetase and GSH increase in quinone-induced oxidative stress in BPAEC. Am J Physiol 1994;267:L414–421. [PubMed: 7943345]
58. Barchowsky A, Roussel RR, Klei LR, James PE, Ganju N, Smith KR, Dudek EJ. Low levels of arsenic trioxide stimulate proliferative signals in primary vascular cells without activating stress effector pathways. Toxicol Appl Pharmacol 1999;159:65–75. [PubMed: 10448126]
59. Barchowsky A, Klei LR, Dudek EJ, Swartz HM, James PE. Stimulation of reactive oxygen, but not reactive nitrogen species, in vascular endothelial cells exposed to low levels of arsenite. Free Radic Biol Med 1999;27:1405–1412. [PubMed: 10641735]

60. Huang HS, Chang WC, Chen CJ. Involvement of reactive oxygen species in arsenite-induced downregulation of phospholipid hydroperoxide glutathione peroxidase in human epidermoid carcinoma A431 cells. Free Radic Biol Med 2002;33:864–873. [PubMed: 12208374]
61. Chan K, Han XD, Kan YW. An important function of Nrf2 in combating oxidative stress: detoxification of acetaminophen. Proc Natl Acad Sci U S A 2001;98:4611–4616. [PubMed: 11287661]
62. McMahon M, Itoh K, Yamamoto M, Chanas SA, Henderson CJ, McLellan LI, Wolf CR, Cavin C, Hayes JD. The Cap'n'Collar basic leucine zipper transcription factor Nrf2 (NF-E2 p45-related factor 2) controls both constitutive and inducible expression of intestinal detoxification and glutathione biosynthetic enzymes. Cancer Res 2001;61:3299–3307. [PubMed: 11309284]
63. Leung L, Kwong M, Hou S, Lee C, Chan JY. Deficiency of the Nrf1 and Nrf2 transcription factors results in early embryonic lethality and severe oxidative stress. J Biol Chem 2003;278:48021–48029. [PubMed: 12968018]
64. Chen L, Kwong M, Lu R, Ginzinger D, Lee C, Leung L, Chan JY. Nrf1 is critical for redox balance and survival of liver cells during development. Mol Cell Biol 2003;23:4673–4686. [PubMed: 12808106]
65. Yang H, Magilnick N, Lee C, Kalmaz D, Ou X, Chan JY, Lu SC. Nrf1 and Nrf2 Regulate Rat Glutamate-Cysteine Ligase Catalytic Subunit Transcription Indirectly via NF-{kappa}B and AP-1. Mol Cell Biol 2005;25:5933–5946. [PubMed: 15988009]
66. He X, Chen MG, Lin GX, Ma Q. Arsenic induces NAD(P)H:quinone oxidoreductase I by disrupting the NRF2/KEAP1/CUL3 complex and recruiting NRF2/MAF to are enhancer. J Biol Chem. 2006
67. Aono J, Yanagawa T, Itoh K, Li B, Yoshida H, Kumagai Y, Yamamoto M, Ishii T. Activation of Nrf2 and accumulation of ubiquitinated A170 by arsenic in osteoblasts. Biochem Biophys Res Commun 2003;305:271–277. [PubMed: 12745069]
68. Bain J, McLauchlan H, Elliott M, Cohen P. The specificities of protein kinase inhibitors: an update. Biochem J 2003;371:199–204. [PubMed: 12534346]
69. Wild AC, Moinova HR, Mulcahy RT. Regulation of gamma-glutamylcysteine synthetase subunit gene expression by the transcription factor Nrf2. J Biol Chem 1999;274:33627–33636. [PubMed: 10559251]
70. Hudson FN, Kavanagh TJ. Cloning and characterization of the proximal promoter region of the mouse glutamate-L-cysteine ligase regulatory subunit gene. Biochim Biophys Acta 2000;1492:447–451. [PubMed: 10899580]
71. Bea F, Hudson FN, Chait A, Kavanagh TJ, Rosenfeld ME. Induction of glutathione synthesis in macrophages by oxidized low-density lipoproteins is mediated by consensus antioxidant response elements. Circ Res 2003;92:386–393. [PubMed: 12600891]
72. Solis WA, Dalton TP, Dieter MZ, Freshwater S, Harrer JM, He L, Shertzer HG, Nebert DW. Glutamate-cysteine ligase modifier subunit: mouse Gclm gene structure and regulation by agents that cause oxidative stress. Biochem Pharmacol 2002;63:1739–1754. [PubMed: 12007577]
73. Chanas SA, Jiang Q, McMahon M, McWalter GK, McLellan LI, Elcombe CR, Henderson CJ, Wolf CR, Moffat GJ, Itoh K, Yamamoto M, Hayes JD. Loss of the Nrf2 transcription factor causes a marked reduction in constitutive and inducible expression of the glutathione S-transferase Gsta1, Gsta2, Gstm1, Gstm2, Gstm3 and Gstm4 genes in the livers of male and female mice. Biochem J 2002;365:405–416. [PubMed: 11991805]
74. McWalter GK, Higgins LG, McLellan LI, Henderson CJ, Song L, Thornalley PJ, Itoh K, Yamamoto M, Hayes JD. Transcription factor Nrf2 is essential for induction of NAD(P)H:quinone oxidoreductase 1, glutathione S-transferases, and glutamate cysteine ligase by broccoli seeds and isothiocyanates. J Nutr 2004;134:3499S–3506S. [PubMed: 15570060]
75. Gong P, Stewart D, Hu B, Vinson C, Alam J. Multiple basic-leucine zipper proteins regulate induction of the mouse heme oxygenase-1 gene by arsenite. Arch Biochem Biophys 2002;405:265–274. [PubMed: 12220541]
76. Sekhar KR, Spitz DR, Harris S, Nguyen TT, Meredith MJ, Holt JT, Gius D, Marnett LJ, Summar ML, Freeman ML, Guis D. Redox-sensitive interaction between KIAA0132 and Nrf2 mediates indomethacin-induced expression of gamma-glutamylcysteine synthetase. Free Radic Biol Med 2002;32:650–662. [PubMed: 11909699]

77. Sekhar KR, Crooks PA, Sonar VN, Friedman DB, Chan JY, Meredith MJ, Starnes JH, Kelton KR, Summar SR, Sasi S, Freeman ML. NADPH oxidase activity is essential for Keap1/Nrf2-mediated induction of GCLC in response to 2-indol-3-yl-methylenequinuclidin-3-ols. Cancer Res 2003;63:5636–5645. [PubMed: 14500406]

78. Yang H, Zeng Y, Lee TD, Yang Y, Ou X, Chen L, Haque M, Rippe R, Lu SC. Role of AP-1 in the coordinate induction of rat glutamate-cysteine ligase and glutathione synthetase by tert-butylhydroquinone. J Biol Chem 2002;277:35232–35239. [PubMed: 12093805]

79. Yang H, Wang J, Huang ZZ, Ou X, Lu SC. Cloning and characterization of the 5′-flanking region of the rat glutamate-cysteine ligase catalytic subunit. Biochem J 2001;357:447–455. [PubMed: 11439094]

80. Harada H, Sugimoto R, Watanabe A, Taketani S, Okada K, Warabi E, Siow R, Itoh K, Yamamoto M, Ishii T. Differential roles for Nrf2 and AP-1 in upregulation of HO-1 expression by arsenite in murine embryonic fibroblasts. Free Radic Res 2008;42:297–304. [PubMed: 18404528]

81. Ishii T, Itoh K, Takahashi S, Sato H, Yanagawa T, Katoh Y, Bannai S, Yamamoto M. Transcription factor Nrf2 coordinately regulates a group of oxidative stress-inducible genes in macrophages. J Biol Chem 2000;275:16023–16029. [PubMed: 10821856]

82. Alam J, Stewart D, Touchard C, Boinapally S, Choi AM, Cook JL. Nrf2, a Cap‘n’Collar transcription factor, regulates induction of the heme oxygenase-1 gene. J Biol Chem 1999;274:26071–26078. [PubMed: 10473555]

83. Yu R, Chen C, Mo YY, Hebbar V, Owuor ED, Tan TH, Kong AN. Activation of mitogen-activated protein kinase pathways induces antioxidant response element-mediated gene expression via a Nrf2-dependent mechanism. J Biol Chem 2000;275:39907–39913. [PubMed: 10986282]

84. Dahl EL, Mulcahy RT. Cell-type specific differences in glutamate cysteine ligase transcriptional regulation demonstrate independent subunit control. Toxicol Sci 2001;61:265–272. [PubMed: 11353135]

85. Zipper LM, Mulcahy RT. Erk activation is required for Nrf2 nuclear localization during pyrrolidine dithiocarbamate induction of glutamate cysteine ligase modulatory gene expression in HepG2 cells. Toxicol Sci 2003;73:124–134. [PubMed: 12657749]

86. Yu R, Mandlekar S, Lei W, Fahl WE, Tan TH, Kong AN. p38 mitogen-activated protein kinase negatively regulates the induction of phase II drug-metabolizing enzymes that detoxify carcinogens. J Biol Chem 2000;275:2322–2327. [PubMed: 10644681]

87. Vaishnav D, Jambal P, Reusch JE, Pugazhenthi S. SP600125, an inhibitor of c-jun N-terminal kinase, activates CREB by a p38 MAPK-mediated pathway. Biochem Biophys Res Commun 2003;307:855–860. [PubMed: 12878189]

88. Dean JL, Sully G, Clark AR, Saklatvala J. The involvement of AU-rich element-binding proteins in p38 mitogen-activated protein kinase pathway-mediated mRNA stabilisation. Cell Signal 2004;16:1113–1121. [PubMed: 15240006]

89. Yang Y, Dieter MZ, Chen Y, Shertzer HG, Nebert DW, Dalton TP. Initial characterization of the glutamate-cysteine ligase modifier subunit Gclm(-/-) knockout mouse. Novel model system for a severely compromised oxidative stress response. J Biol Chem 2002;277:49446–49452. [PubMed: 12384496]

90. Chen Y, Shertzer HG, Schneider SN, Nebert DW, Dalton TP. Glutamate Cysteine Ligase Catalysis: DEPENDENCE ON ATP AND MODIFIER SUBUNIT FOR REGULATION OF TISSUE GLUTATHIONE LEVELS. J Biol Chem 2005;280:33766–33774. [PubMed: 16081425]

91. Lee JI, Kang J, Stipanuk MH. Differential regulation of glutamate-cysteine ligase subunit expression and increased holoenzyme formation in response to cysteine deprivation. Biochem J 2006;393:181–190. [PubMed: 16137247]

92. Dasgupta A, Das S, Sarkar PK. Thyroid hormone promotes glutathione synthesis in astrocytes by up regulation of glutamate cysteine ligase through differential stimulation of its catalytic and modulator subunit mRNAs. Free Radic Biol Med 2007;42:617–626. [PubMed: 17291985]

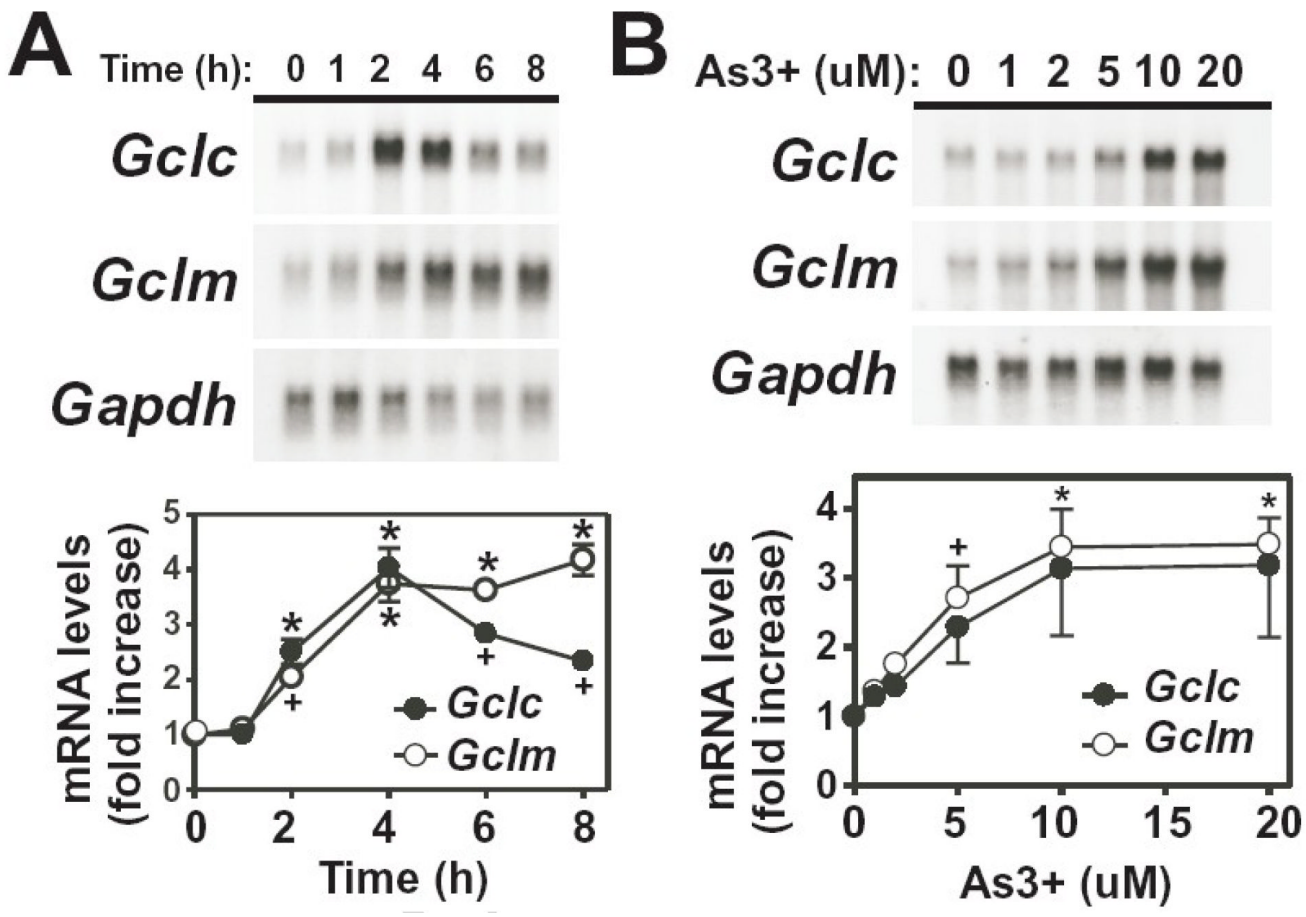

Figure 1. Time- and dose-dependent induction of *Gclc* and *Gclm* expression by As3+

(A) TAMH cells were treated with As3+ (10 μM) for the time periods indicated. (B) TAMH cells were treated for 4 h with the indicated concentrations of As3+. Total RNA was isolated and relative mRNA levels were analyzed by Northern blotting as described in the Methods section. *Gclc* (closed circles) and *Gclm* (open circles) expression was normalized to *Gapdh* mRNA levels and the graphical data presented are averages +/− SEM of at least three experiments. $+p < 0.05$ and $*p < 0.001$, indicates a significant difference compared to untreated control.

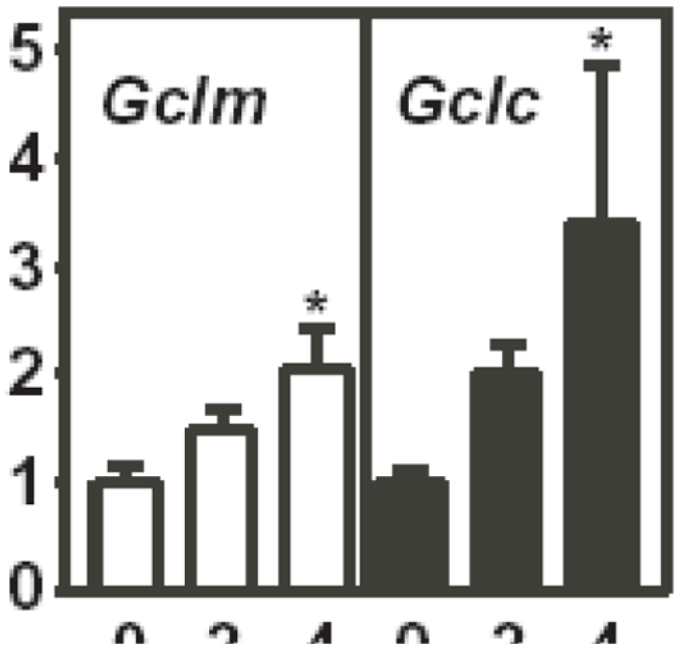

Figure 2. As3+ increases the rate of transcription of *Gclc* and *Gclm*

TAMH cells were treated with 10 μM As3+ for the time periods indicated. Nuclei were isolated and nuclear run-on analysis was performed as described in the Methods section. Relative rates of transcription of *Gclm* (open bars) and *Gclc* (closed bars) were quantitated and normalized to *β-Actin*. The data presented are averages +/− SEM of three experiments. *$p < 0.05$, indicates a significant difference compared to untreated control.

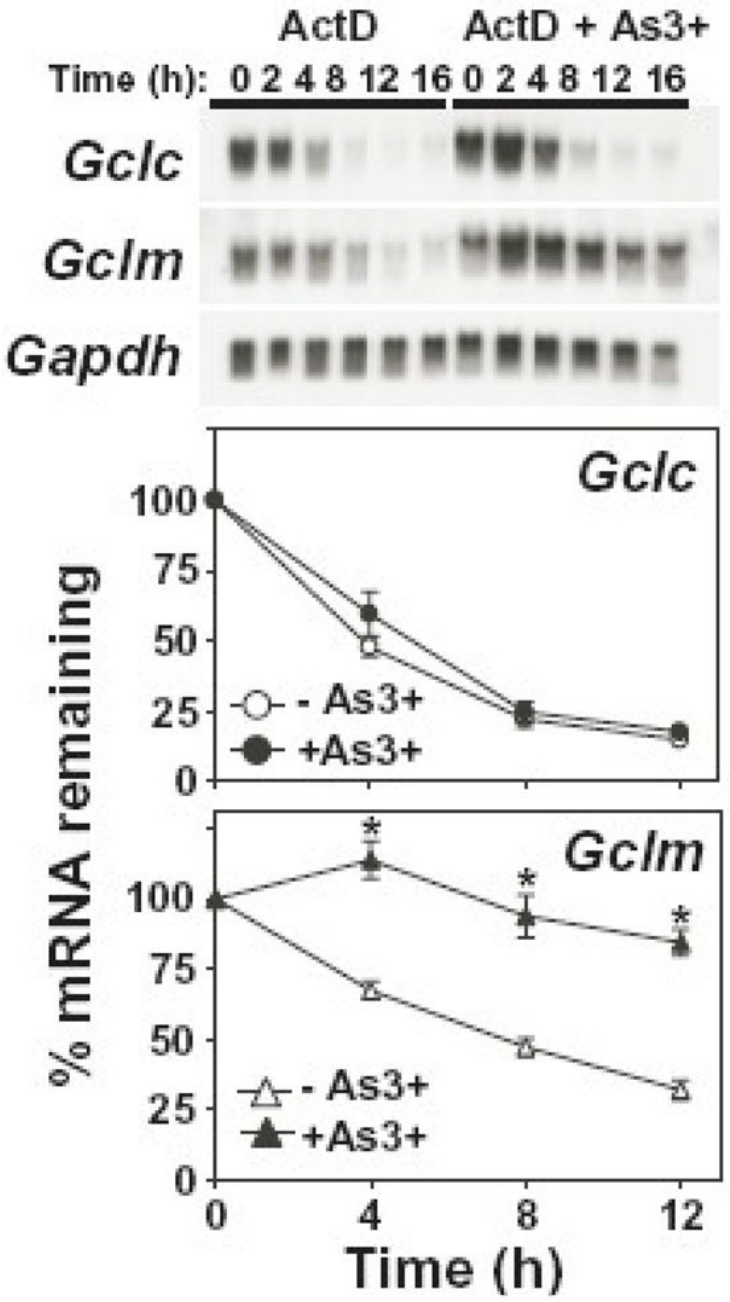

Figure 3. As3+ induces the post-transcriptional stabilization of *Gclm* mRNA

TAMH cells were treated with actinomycin D (ActD; 500 ng/ml) in the absence (open symbols) or presence (closed symbols) of As3+ (10 μM) for the time periods indicated. Relative mRNA levels were analyzed by Northern blotting. *Gclc* (circles; upper panel) and *Gclm* (triangles; lower panel) expression was normalized to *Gapdh* mRNA levels and the graphical data presented are averages +/− SEM of seven experiments. *$p < 0.01$, indicates a significant difference compared to ActD alone at that time point.

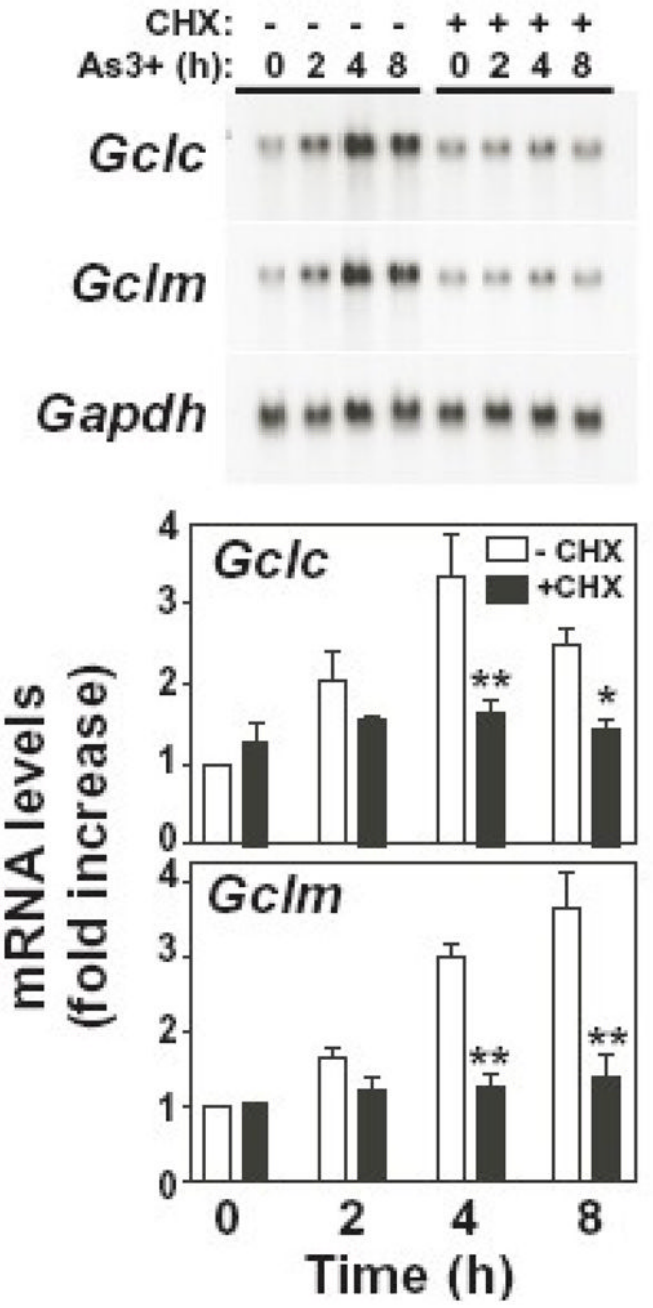

Figure 4. *de novo* protein synthesis is required for As3+-induced *Gclc* and *Gclm* expression

TAMH cells were preincubated in the absence (open bars) or presence (closed bars) of cycloheximide (CHX; 1.0 μg/ml) for 1 h prior to treatment with As3+ (10 μM) for the time periods indicated. Relative mRNA levels were analyzed by Northern blotting. *Gclc* (upper panel) and *Gclm* (lower panel) expression was normalized to *Gapdh* mRNA levels and the graphical data presented are averages +/− SEM of three experiments. **p* < 0.05 and ***p* < 0.001, indicates a significant difference compared to As3+ alone at that time point.

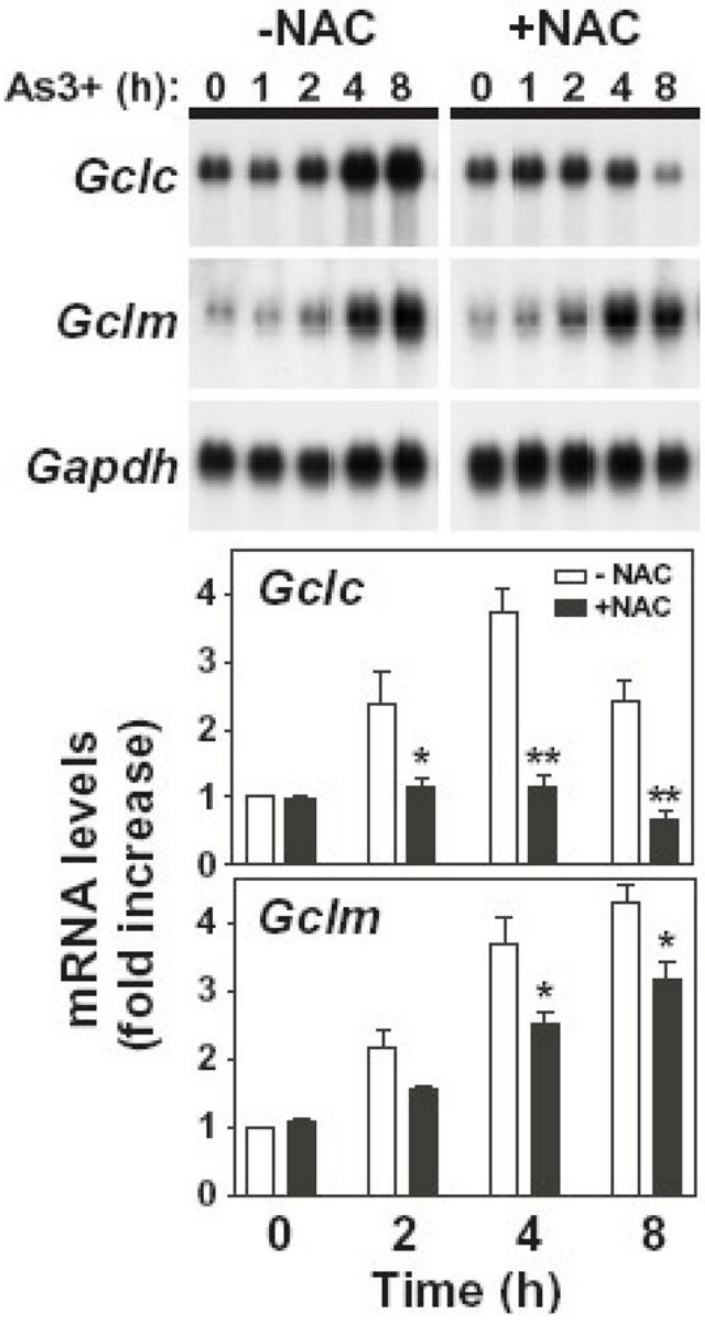

Figure 5. Differential regulation of As3+-induced *Gclc* and *Gclm* expression by N-acetylcysteine

TAMH cells were preincubated in the absence (open bars) or presence (closed bars) of N-acetylcysteine (NAC; 10 mM) for 1 h prior to treatment with As3+ (10 μM) for the time periods indicated. Relative mRNA levels were analyzed by Northern blotting. *Gclc* (upper panel) and *Gclm* (lower panel) expression was normalized to *Gapdh* mRNA levels and the graphical data presented are averages +/− SEM of three experiments. **p* < 0.05 and ***p* < 0.001, indicates a significant difference compared to As3+ alone at that time point.

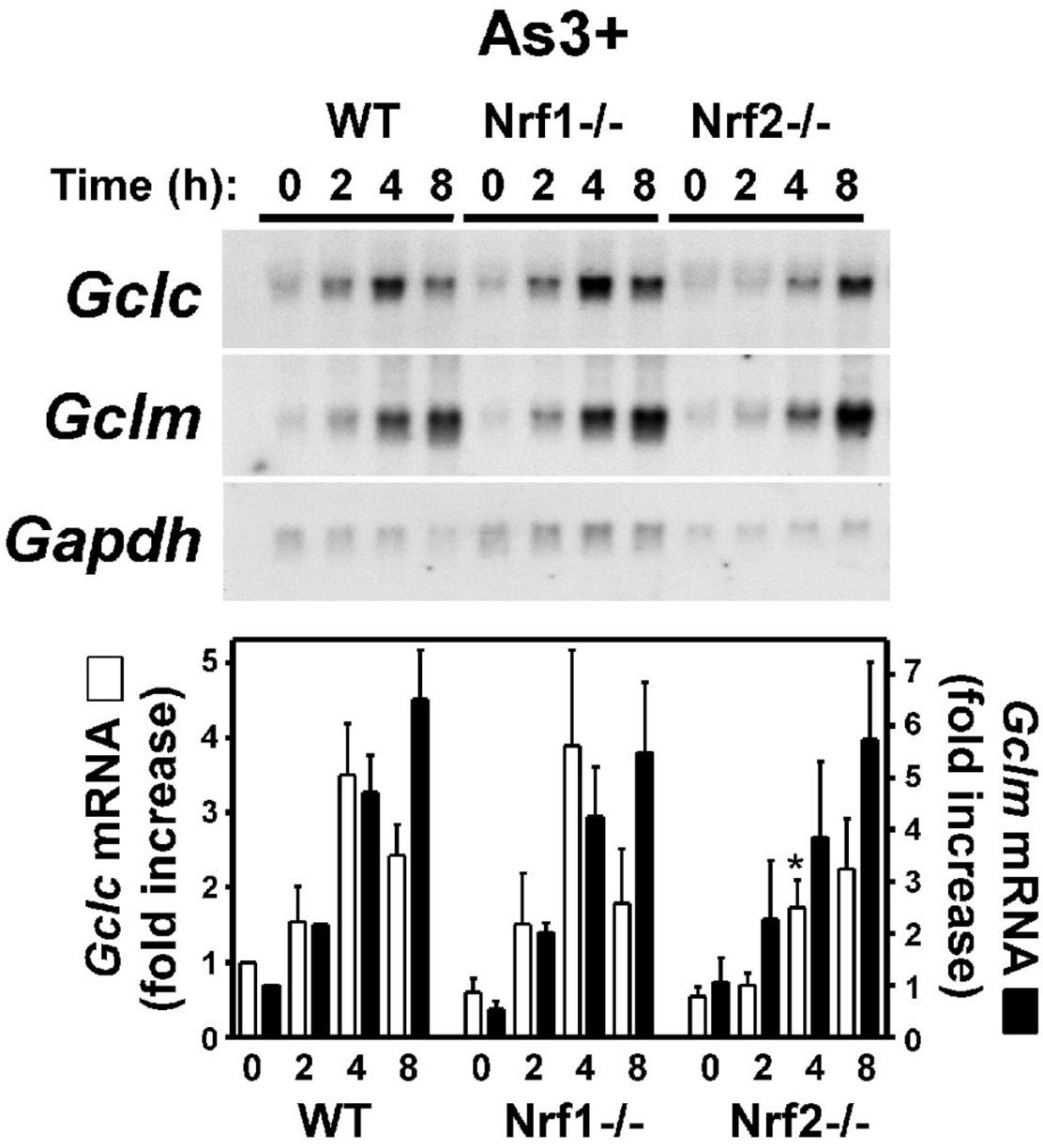

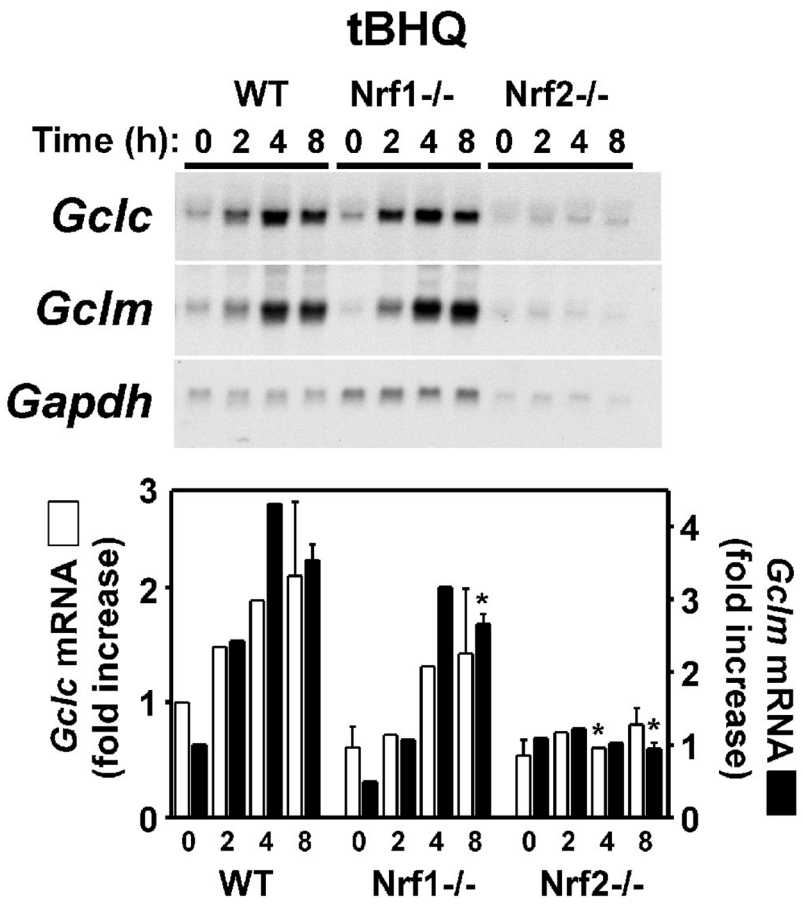

Figure 6. As3+ induces *Gclc* and *Gclm* expression independent of Nrf1 or Nrf2

MEFs from WT, Nrf1(−/−), or Nrf2(−/−) mice were treated with (A) As3+ (10 μM) or (B) *tert*-butylhydroquinone (tBHQ; 30 μM) for the time periods indicated. Relative mRNA levels were analyzed by Northern blotting. *Gclc* (open bars) and *Gclm* (closed bars) expression was normalized to *Gapdh* mRNA levels and the graphical data presented are averages +/− SEM of at least three experiments. *$p < 0.05$, indicates a significant difference compared to As3+-induced gene expression in WT MEFs at that time point.

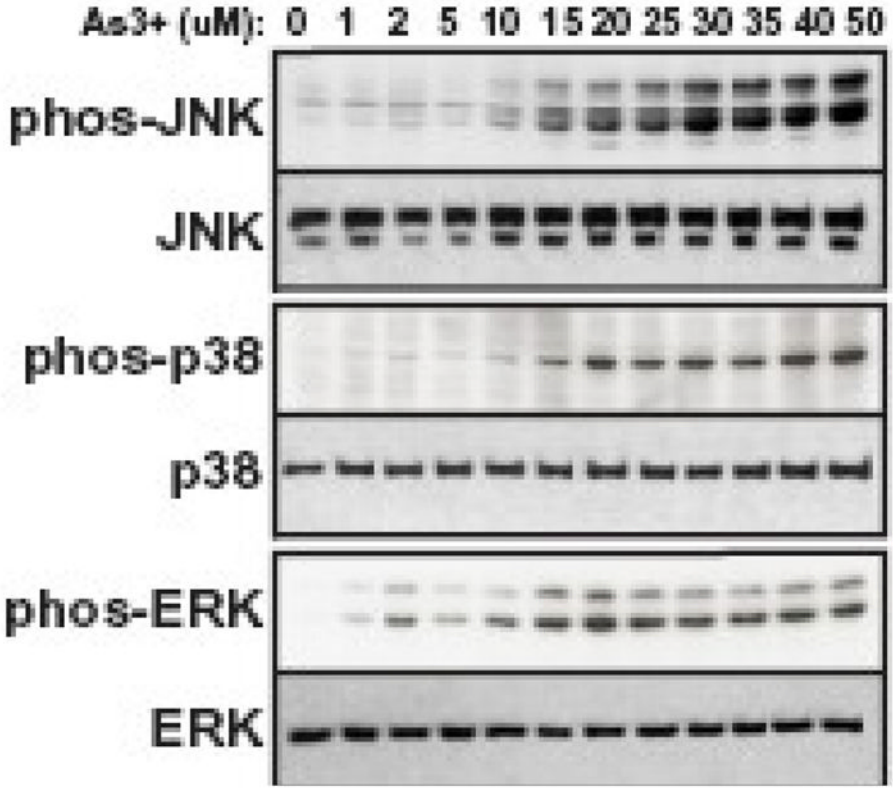

Figure 7. Dose-dependent As3+-induced MAPK activation in TAMH cells

TAMH cells were treated for 4 h with the indicated concentrations of As3+ and JNK, p38 and ERK phosphorylation analyzed by immunoblotting using phospho-specific antibodies as described in the Methods section. The two bands recognized by the p-JNK and p-ERK antibodies are the p46 and p54 JNK family isoforms and p44 ERK1 and p42 ERK2, respectively. Total MAPK protein expression was assessed by immunoblotting using antibodies against JNK, p38 MAPK, and p42 ERK2. The p42 ERK2 antibody does not readily detect p44 ERK1 resulting in a single immunoreactive band.

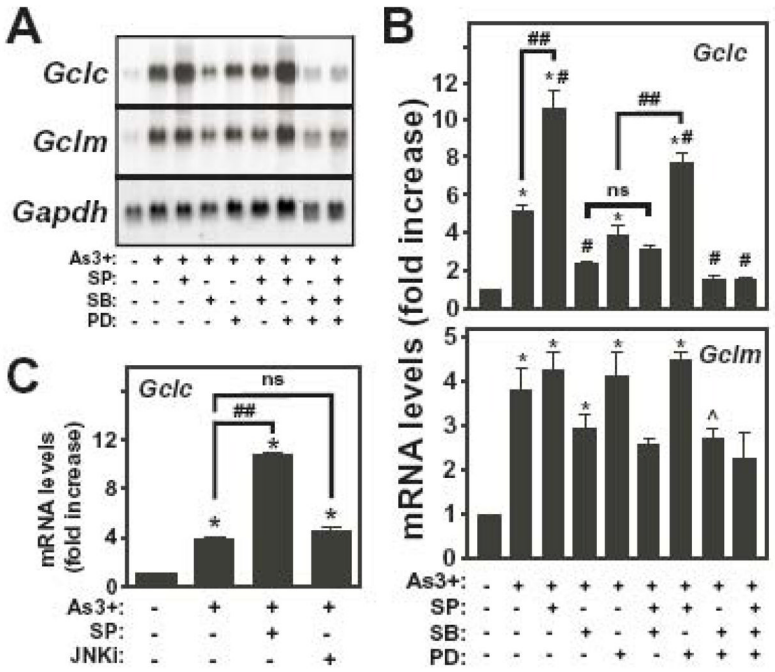

Figure 8. Role of MAPKs in As3+-induced *Gclc* and *Gclm* expression

TAMH cells were preincubated with SP600125 (SP; 25 μM), SB202190 (SB; 5 μM), and/or PD98059 (PD; 25 μM), or JNKi (20 uM) for 1 h prior to treatment with As3+ (10 μM) for 4 h as indicated. (A) Relative mRNA levels were analyzed by Northern blotting. (B) *Gclc* (upper panel) and *Gclm* (lower panel) expression was normalized to *Gapdh* mRNA levels and the graphical data presented are averages +/− SEM of at least four experiments. (C) *Gclc* and *β-Actin* mRNA levels were determined by real-time RT-PCR. *Gclc* mRNA levels were normalized to *β-Actin* and presented as fold increase over untreated control. **p* < 0.001 and ^p < 0.05, indicates a significant difference compared to untreated control. #*p* < 0.05, indicates a significant difference compared to As3+ alone. ##*p* < 0.05, indicates a significant difference in the presence of SP600125.

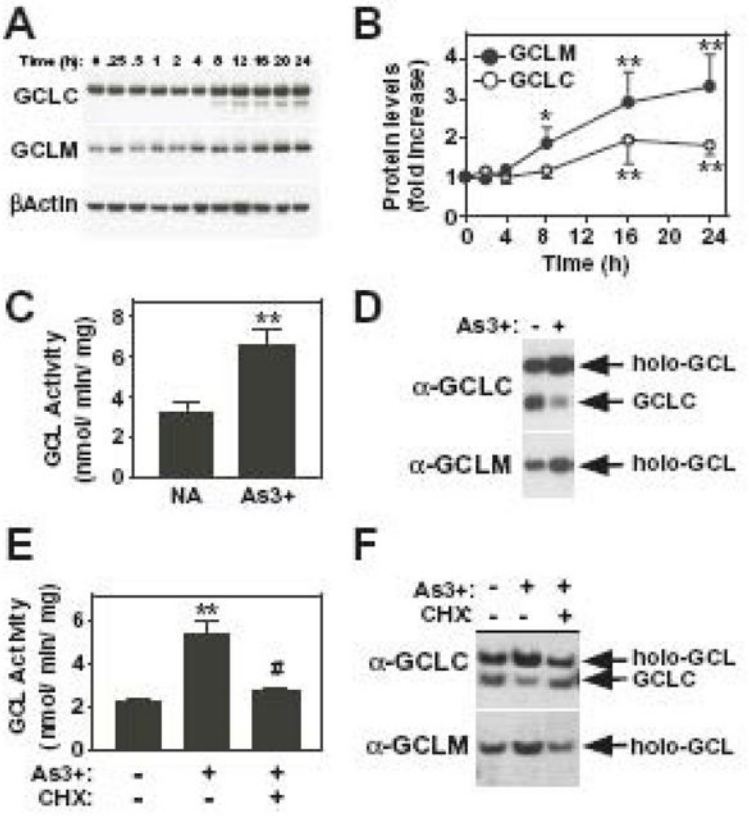

Figure 9. As3+ increases GCL subunit protein levels, GCL activity and holoenzyme formation

(A and B) TAMH cells were treated with As3+ (10 μM) for the time periods indicated. (A) GCLC, GCLM, and βActin protein expression were analyzed by denaturing SDS-PAGE and immunoblotting as described in the Methods section. (B) Graphical presentation of the studies described in (A). GCLC and GCLM protein expression were normalized to βActin protein levels and the data presented are averages +/− SEM of at least four experiments. (C–F) TAMH cells were preincubated in the absence or presence of cycloheximide (CHX; 1.0 μg/ml) for 1 h prior to treatment with As3+ (10 μM) for 16 h as indicated. (C and E) Cells were harvested and extracts assayed for GCL enzymatic activity as described in the Methods section. The graphical data presented are averages +/− SEM of 3–7 experiments. (D and F) GCL holoenzyme formation was analyzed by native gel electrophoresis and immunoblotting for GCLC or GCLM as described in the Methods section. *$p < 0.05$ and **$p < 0.01$, indicates a significant difference in protein expression or activity compared to untreated control. #$p < 0.01$, indicates a significant difference in GCL activity compared to As3+ alone.